The Spatial Distributions of Mineralisation.

Bruce E. Hobbs, Alison Ord and Thomas Blenkinsop.

Abstract.
The concept of fractal spatial distributions of mineralisation has been widely proposed since Mandelbrot (1965) who emphasised the stable Pareto-Lévy distribution as the relevant distribution. The concept of a fractal is used as a basis for estimating endowment and for erecting exploration models based on self-organised criticality. This paper explores the proposition that the growth kinetics for a mineralising system are reflected in the probability distributions that describe the spatial patterns of mineralisation. We revisit the data sets and ask the question: *What are the best fit probability distributions for the spatial distribution of mineralisation*? The answer is: *members of the Extreme Value Distribution family* (*Gumbel-, Fréchet- and Weibull- distributions*) *and not the Pareto distribution.* Thus, the spatial distribution of mineralisation is not a fractal although the tails of the distributions can be or resemble power-laws. The standard box counting procedure for a spatial point distribution establishes a nearest neighbour distribution and hence, by definition, the resulting distribution is Weibull and not Pareto. The mass distributions are Fréchet and not Pareto. The extreme end members are Gumbel. We discuss the implications of these distributions for models that generate mineralisation sites within a system and for the underlying thermodynamics.
Keywords: *Fractals, Generalised Extreme Value (GEV) distributions, Fréchet-, Weibull-, Gumbel-distributions, box counting, nearest neighbour-distributions, mineralisation growth models.*

1. Introduction.

This paper concerns process probability distributions based on the processes that generate mineralisation and that characterise the spatial distribution of mineralisation at the regional scale. The emphasis is on orogenic gold deposits. The spatial distribution at all length scales is intrinsically heterogeneous and there are a number of ways of characterising such heterogeneity. One way is to use correlation functions of various kinds (Kroner, 1971; Torquato, 2002; Kalidindi, 2015); this commonly employs Fourier transforms to establish *n*-point correlation functions (Kalidindi, 2015). A second way is to use wavelet transforms (Arneodo et al., 1995) in association with Hurst exponents (Ord et al., 2016; Munro et al., 2018; Doutre et al., 2015; Doutre, 2018) to establish spatial patterns, correlations and multi-fractal spectra. A third way is to establish the recurrence patterns and associated quantitative measures for the system (Ord et al., 2018; Hobbs and Ord., 2021). Another is to establish the probability functions that characterise the heterogeneity. This paper concentrates on the latter. Although all four methods have a thermodynamic underpinning (Beck and Schlögl, 1995; Arneodo et al., 1995), the statistical functions are directly related to the thermodynamics of the system (Lavenda, 1995) and hence place important constraints on models for the formation of the mineralisation. In fact all four approaches are related through the attractor for the system. The attractor is the *N*-dimensional topological surface (which can be fractal) that describes the geometry of physical and chemical states that the system can occupy (Sprott, 2003). *N* is the number of independent degrees of freedom for the system. Nonlinear systems involving similar physical and chemical processes evolve with time towards similar attractors for a large range of initial conditions. The attractor is characterised by many quantitative measures: The large number of (in principle, indefinite) states on the attractor of a nonlinear system gives rise to the multifractal nature of the system (Beck and Schlögl, 1995) together with the observed probability distributions (Lucarini et al., 2016). Recurrence arises from the system repeatedly visiting neighbouring states on the attractor (Marwan et al., 2007). The correlations measure how the states on the attractor for the system are inter-related (Sethna, 2006, Chapter 10). The probability distributions are measures of the geometry of the attractor (Lucarini et al., 2016; Bodai, 2016).

A quote from Savageau (1979) illustrates the concept explored in this paper: *Any system that grows into a stable mature form has a growth curve that is a legitimate cumulative probability distribution*. Hence the observed probability distributions not only contain information on the geometry of the attractor resulting from the nonlinear dynamics of a mineralising system but have the potential to constrain the growth kinetics of the mineralising system.

Traditionally, two empirical probability distributions have been used to characterise mineralisation patterns. These are the log-normal (Singer, 2013; Singer and Menzie, 2010) and the power-law (Mandelbrot, 1965) distributions although only the latter are commonly used for spatial patterns of mineralisation. The power-law distribution is written:

$$N(r) = Ar^{-D} \qquad (1)$$

where $N(r)$ is the number of boxes or spheres with dimension, r, occupied by mineralisation sites in a region of interest, A is a constant and D is a characteristic *power law exponent*, commonly referred to as the *fractal dimension*. Although power law behaviour is implied explicitly by many authors, such behaviour can commonly be demonstrated over only a limited range in r (Kruhl, 2013) and commonly is an approximate fit to the data (Corral and Gonzalez, 2019). (1) is known as a *power-law distribution* (physics), a *Pareto distribution* (finance), a *hyperbolic distribution* (social sciences) and as a stable[1] *Pareto-Lévy distribution* (Mandelbrot, 1960, 1961, 1963). These distributions have been popular because they have simple mathematical expressions and have heavy right hand tails so that considerable departures from the sample mean can be accommodated. In particular the Pareto-Lévy distribution was favoured by Mandelbrot (see Appendix 1) because he showed it was able to characterise considerable volatility (departures from the mean) in commodity and financial markets. Both he and Fama (1963, 1965) identified the Pareto distribution as a best fit for the data, capable of accommodating skewness and the slowly decaying tails of the empirical distributions. It is clear though that Fama (1965) was aware of the Generalised Extreme Value (GEV) distributions studied by Tippet (1925), Gnedenko and Kolmogorov (1968) and Gumbel (1954). Mandelbrot (1956) refers to the work of Gnedenko and Kolmogorov (1968) but does not follow up on the extreme distributions. The GEV distributions are the topic of this paper.

[1] A probability distribution is said to be *stable* if linear combinations of that distribution add together to produce the same kind of distribution. The stable distributions are the Gaussian, Cauchy, Lévy, Gumbel, Weibull and Fréchet distributions (Nair et al., 2021).

We note that although both the log-normal and power law distributions have heavy right handed tails only the log-normal distribution has a well-defined mean and variance so that the mean of the (logarithm of) observations tends to the mean of the distribution with increasing numbers of observations as defined by the Law of Large Numbers (Dekking, 2005, p181 - 190). In contrast, the power-law distribution lacks a mean or variance and the sample arithmetic mean diverges as the number of observations increases.

In this paper we show that the GEV distributions characterise the spatial distribution of mineralisation far better than the Lévy-Pareto distribution. Moreover, not only do the GEV distributions arise directly from the Generalised Central Limit Theorem, they have a strong foundation in thermodynamics and arise directly both from realistic growth laws for mineralising systems and from the nonlinear dynamics of these systems.

The structure of this paper is as follows. In Section 2, we examine the statistical basis for and the overall characteristics of the GEV distributions. In Section 3 we give examples of spatial distributions for mineralisation that have formerly been interpreted as fractal (or bi-fractal) distributions and show that they are better represented as GEV distributions rather than the traditional Pareto distributions. In Section 4 we consider the thermodynamic basis for GEV distributions and indicate the significance for mineralising systems. Basically the generation of GEV distributions for a mineralising system is an expression of the partitioning of energy that has been input to the open system. We also show that realistic growth models for mineralising systems lead to GEV distributions for the spatial arrangement of mineralising sites within a system. We also indicate some directions for future work and point to alternative distributions that may characterise mineralised systems other than orogenic gold deposits. Finally we draw some conclusions in Section 5.

2. Probability distributions for mineralising systems.

We would like an understanding of the statistics that result from the various processes that operate in mineralising systems with the perhaps optimistic view that the measured statistics of such systems may improve predictability, discovery and extractability, and provide constraints on the processes that operated to form these systems. To this end we seek an understanding of the observed probability distributions in terms of physical and chemical processes and if possible of thermodynamics rather than pragmatic statements regarding the class of probability distribution displayed, such as log-normal or Pareto, with no associated physical, chemical or geological insight. Interestingly, we find that log-normal and fractal (Pareto Type I; See https:// reference.wolfram.com/language/ref/ParetoDistribution.html for usage.) distributions play only subsidiary roles in this framework despite the wide emphasis on such distributions in the literature. In order to progress and understand any relationship to the processes involved in mineralisation we need to look at the physical basis for many of the distributions used in the literature.

In advance, we present in Table 1 Appendix 2 some of the probability distributions of interest with respect to spatial distributions along with their associated physical processes and constraints that result in the distribution maximising entropy. For details see Frank (2009, 2019).

2.1. Closed systems at equilibrium.

In closed systems at equilibrium the entropy is maximised (Gibbs, 1875-1878; Callen, 1960). Thus the governing principle for such systems is that the processes that lead to equilibrium produce probability distributions that maximise the entropy. Other constraints also maximise the entropy for other distributions. There is a zoo of statistical functions (see: https://en.wikipedia.org/wiki/Relationships_among_probability_distributions and https://www.itl.nist.gov/div898/handbook/eda/section3/eda366.htm). The classical approach has been to select the simplest of these, namely the Gaussian distribution, the log-normal distribution or the power-law and to regard any other kind of distribution as something pathological. See Appendix 3 for further details.

2.2. Open systems far from equilibrium.

There is of course an enormous range of distributions other than those considered above and in Appendix 2 but few have any thermodynamic basis or seem capable of reflecting the processes that operate during the formation of the systems involved. It is important to note that the Gaussian, log-normal and Boltzmann distributions are relevant to isolated systems or closed systems in contact with a heat bath; all such systems are at equilibrium. However, mineralising systems, while they operate, are far from equilibrium and are open systems (Ord et al., 2012). It seems logical that the distributions in Section 2.1 may not be relevant to open systems far from equilibrium and we ask: *what statistical distributions might be relevant to far from equilibrium systems where variables are not independent of each other and both long and short range interactions and correlations exist*? Such systems are commonly characterised by long, fat tails where the mean of the distribution diverges as the sample size increases and the variance may be infinite. Some of these distributions are classified in Figure 1 which distinguishes distributions according to the nature of the tails of the distributions. If the tails approach a power law for large populations they are said to be *regularly varying*. There are many distributions in this category other than the Pareto distribution which is distinguished by being also scale invariant.

2.3. Spatial point distributions.

The traditional box counting procedure in two dimensions for an array of points consists of scanning the array with a series of “boxes” (circles or squares) with varying dimension, *r*, and counting the number, $N(r)$, of boxes that contain at least one point for each value of *r*. If $N(r)$ is related to *r* by (1) then $N(r)$ follows a power law and fractal geometry is implied with a fractal dimension, *D*. The normal procedure is to plot log $N(r)$ against log *r* and if a straight line ensues the geometry of the point array is implied to be fractal. The following argument follows Blenkinsop and Sanderson (1999). If the sampling of points is a Poisson process so that *n* boxes are distributed randomly over the space then the probability of a box containing *x* points is

$$P(x) = \frac{\lambda^x}{x!}\exp(-\lambda)$$

where λ is the mean number of points per box.

The probability of a box containing at least one point is (remembering that 0! = 1)

$$P(x \ge 1) = 1 - P(0) = 1 - \exp(-\lambda)$$

If we take $\lambda = nr^2$ (Blenkinsop and Sanderson, 1999) then

$$P(x) = 1 - \exp\left(-nr^2\right) \quad (1)$$

which is the equation for a cumulative Weibull distribution with $\gamma = 0.5$. The corresponding probability density distribution is

$$G(x) = 2nx\exp\left(-nx^2\right) \quad (2)$$

This distribution is illustrated in Figure 2 for the number of mineralised sites, $n = 1000$, and a square sample area 1000 km across. The result is a curve that could be fitted by two linear regions representing two fractal dimensions, one at spatial scales below 100km and the other at larger spatial scales. This is the kind of interpretation made by Raines (2008) with respect to the data of Agterberg et al. (1993, Table 1). .

The traditional box counting procedure for a two dimensional array of points is in fact a means of calculating a nearest neighbour distribution (Cressie, 1993, his Figure 8.9) which is known to be a Weibull distribution (Chandrasekhar, 1943; Lavenda, 1995, pp 164, 182; Carpena and Coronado, 2019). This distribution closely resembles a Pareto distribution for small values of α but for large values of α might be interpreted as a *bifractal* distribution (Figure 2) as does Blenkinsop (1994), Carlson (1991) and many others for their data sets. Hodkiewicz et al. (2005) document fractal distributions of damage in the Yilgarn of WA. Fractal dimensions vary between 1.5 and 1.9. It would be interesting to test if this is an expression of a Weibull nearest neighbour distribution as predicted by theory.

Carpena and Coronado (2019) show that if the probability distribution of spacings, s, between consecutive members of a point set is $P(s)$ [this is the nearest neighbour distribution] then the box counting dimension, D_{box}, is related to $P(s)$ by

$$P(s) \sim s^{-(1+D_{box})} \quad (3)$$

so that

$$D_{box} = -\left(1 + \frac{\log P(s)}{\log s}\right) \quad (4)$$

Thus D_{box} is a constant only if log $P(s)$ is a linear function of log s otherwise the spatial distribution is not a fractal

This means that if the nearest neighbour distribution is a power law (albeit perhaps only over a limited range) then the data are fractal (over that range) and D_{box} can be defined. Otherwise the data are not fractal. It is possible then to define a fractal dimension at each point in the distribution; this is called a *local fractal dimension*. Further discussion in some detail is in Carpena and Coronado (2019, p 02205-3).

3. Examples of mineralised systems.

In this section we take the data from three well documented examples (Agterberg, 2013; Blenkinsop and Sanderson, 1999 and Blenkinsop, 2014) that have been discussed in terms of fractal (or power-law) distributions and reconsider them in terms of best fit probability distributions: in all cases these turn out to be extreme value distributions.

3.1. Example from Kirkland Lake, Canada.

The first example is from Agterberg (2013, his Figure 4) and is a reprocessed version of data given in Raines (2008) where the interpretation was that the data are bi-fractal. Agterberg considers that the nonlinear distribution is a roll-off effect and fits a line with slope 1.528 to these data in a log-log plot (Figure 3a). These same data on a linear-linear plot are shown in Figure 3(b) with a power-law fit shown. One sees that the entire data set can be represented with a power-law exponent of 1.206 whereas Agterberg (2014) fits eight data points to a power law with exponent 1.528. As indicated, Raines (2008) proposed a bi-fractal fit to these data. An attempt to fit two Pareto distributions to the data of Figure 3(a) using Mathematica (Wolfram Research 2020) failed. Results for a single Pareto fit are moderately good as suggested by Figure 3(b) and are given in Figure 4.

These same data are shown in Figure 3(c) as a log-log plot where a good parabolic fit is shown. Figure 3(d) shows the local box-counting dimension calculated from (4). One sees that values close to that proposed by Agterberg for D_{box} are obtained only for the last two data points. Most values are greater than two and hence are physically unrealistic. The conclusion is that for this example, the nearest neighbour distribution, $P(s)$, is not fitted well by a power law (although Figure 3b looks good to the eye) and the data set is not a fractal. In fact the data set is well fitted by a Weibull distribution (Figures 3 e, f) as is expected of a nearest neighbour distribution.

From a purely pragmatic view of the Agterberg data set, another distribution (the gamma distribution) is just as likely as the Weibull distribution. In order of fit, Mathematica (Wolfram Research 2020) identifies and ranks the distributions in Table 1 where a value of 1.0 is a perfect fit and zero means Mathematica cannot find a fit. The fit for a gamma distribution is shown in Figure 5 for comparison with Figures 3 (e and f). The fit for a single Pareto distribution (Figure 4) is moderate. Notice that the distribution in Figure 4 is a Pareto Type II distribution and not the power-law Pareto Type 1 distribution.

3.2.Spatial data from Zimbabwe.

The second example is from Blenkinsop and Sanderson (1999) and consists of spatial distribution data from the Zimbabwe craton. Log-log plots of $N(r)$ against r are nonlinear (Figure 6) similar to the Agterberg data in Figure 3 (a, c). This nonlinearity reduces the estimated fractal dimension and is interpreted by Blenkinsop and Sanderson (1999) as a roll-off effect.

In Figure 7 we show best fit distributions to the Blenkinsop and Sanderson spatial data. Mathematica (Wolfram Research 2020) chooses a Weibull distribution as best fit for most situations. The exception is the Shamva data set where the best fit is a Gumbel distribution.

3.3. Mass data from Zimbabwe.

The third example (from Blenkinsop, 2014, his Figure 7) consists of mass distributions (Figure 8) as well as probability distributions (Figures 9 and 10) for some of the Zimbabwe examples given above in example 2.

4. Discussion.

4.1. Growth and probability distributions.

Section 3 has considered spatial-point and spatial-mass data sets from two different locations. In each case the spatial data sets conform to a Weibull distribution rather than a Pareto. This is to be expected since the standard box counting procedure for spatial data points is a way of determining a nearest neighbour distribution which is by definition a Weibull distribution. The spatial-mass distributions are Fréchet or Weibull distributions.

Analysis, using Carpena and Coronado (2019), shows that the underlying spatial distributions are not fractal-like. In this section we attempt a rationalisation of these observations in terms of the probability distributions to be expected from the growth of a mineralising system.

Consider a deforming segment of the Earth's lithosphere that is subjected to energy and mass input in the form of hot reactive fluids bearing dissolved metals (Figure 11). We suppose the deformation takes place by brittle processes that generate increased permeability. At these sites energy is further dissipated by the initiation of mineral reactions that result in alteration and mineralisation. The question is: *What controls the spatial distribution of mineralising sites which in this context we identify with sites where the energy input to the system is dissipated*?

Both heterogeneity and anisotropy have important influences on the development of models for point patterns (Moller and Toftaker, 2014) but as far as we are aware such effects have not been considered in the geological literature. We consider only the published data on the distribution of mineralisation; anisotropy and heterogeneity are issues to be considered in the future.

In classical statistical thermodynamics, Boltzmann statistics describes the energy partitioning in an isolated system and for a system in contact with a heat bath. This arises because the partition of an isolated thermodynamic system into a number of components at equilibrium leads to sharing of the system's energy in such a way that the most probable value of the energy of any component is the mean value of the energy. The result is a Boltzmann distribution in three dimensions or a Rayleigh distribution in two dimensions. However for an open system far from equilibrium the internal entropy decrease associated with the ordering represented by the spatial patterning of energy leads to stable extreme distributions where there is an overwhelming probability for one component to take a much larger share of the energy than all others. The distribution of energy now follows an arcsine distribution (Mandelbrot, 1956; Lavenda and Florio, 1992; Lavenda, 1995, pp 11 -15, 80 - 83) and can also be described by one of the Extreme Value probability distributions. The distribution represented in any particular situation is a function of the growth mechanisms associated with energy dissipation. For instance, if there is some kind of cut off with respect to the stress required for fracture propagation (as there is in the classical Griffith theory of fracture; Lavenda, 1965, p 180) a Weibull distribution is expected for stress sites and a Fréchet distribution for fracture length (Lavenda, 1965, p 180). We explore such concepts below in terms of the growth of a mineralising system from the initial input of energy to the dissipation of this energy by the formation of alteration and mineralising sites to the final extinction of the system due to a lack of supply of energy (heat or fluid) to the system or depletion in reactive components.

The following discussion is motivated by the observations of Savageau (1979, 1980), Frank (2009, 2019) and Rocha and Aleixo (2013) that the cumulative probability distribution for a quantity, X, reflects aspects of the curve that characterises the growth kinetics of X. In addition, Nair et al. (2021, Chapter 5) show that non-equilibrium conditions ("external influences") are necessary to generate members of the generalised extreme value family. Savageau (1979, 1980) show that for interacting nonlinear systems, a general equation can be derived that describes the generation of a quantity of interest, X, and competition with other processes to produce a generalised growth law for X. This equation includes many of the common growth laws (logarithmic, power law, Weibull, stochastic, Gompertz and Lotka-Volterra) as special cases. His analysis emphasises that although a large number of processes may operate to produce the growth of a system, an overall simple pattern of growth may result.

A process oriented discussion of the significance of the three stable extreme distributions is given by Rocha and Aleixo (2013). That paper (although directed at the growth of tumours) provides a model for the growth of a mineralising system or any other system growth that comprises nucleation, growth and extinction phases. The model is relevant at all scales so we expect it to be applicable to the regional scale for the distribution of metal endowment and at smaller scales where one is concerned with the distribution of alteration assemblages or of ore grade in a single deposit or for the spatial distribution of mineralisation.

Rocha and Aleixo (2013) explore a generalised growth model that describes the progressive evolution of a system where growth nucleates, and subsequent growth follows a symmetrical or asymmetrical sigmoidal curve to ultimate extinction. This is the Gompertz law:

$$f_{r,q,p}\left(x\right) = rx^{p-1}(1-x)^{q-1}$$

which is a generalisation of the simple logistic equation, widely used in population dynamics, for which $q = p = 2$. The logistic equation was used as an empirical fit by Hubbert (1962) to the rates of discovery and production of oil resources and thus to predict peak oil; this concept has since been extended to other resources including gold (e.g. Bardi and Lavacchi, 2009). The Gompertz law describes the competition between an accelerating growing process and processes that tend to inhibit growth; it is attractive from a process point of view since it is used in various forms in material science (in the form of Kolmogorov–Avrami kinetics for recrystallisation; Martyushev and Axelrod, 2003) and as a form of kinetics for non-equilibrium chemical systems with coupling to both heat and fluid supply (Ord et al., 2012; Hobbs and Ord, 2018). It is also one member of the more general growth laws discussed by Savageau (1979, 1980)

With the approximation, $\ln(x) \approx -(1-x)$ for $0 \le x \le 2$, and t a normalised time, Rocha and Aleixo show that the Gompertz law can be expressed as

$$\frac{df_N\left(t\right)}{dt} = bf_N\left(t\right)^{p-1}\left(-\ln f_N\left(t\right)\right)^{q-1}$$

With $p = 2$ and $1 < q < 2$, this equation leads to Weibull distributions. If $p = 2$ and $q > 2$ then Fréchet distributions result. For $b = 1$, the Weibull distributions are of the form

$$f_N\left(t\right) = \exp\left(-(-t)^{\alpha}\right) \text{ with } 0 < \frac{1}{\alpha} < 1$$

The Fréchet distributions are of the form

$$f_N\left(t\right) = \exp\left((-t)^{-\alpha}\right) \text{ with } \frac{1}{\alpha} > 0$$

Plots of these distributions are shown in Figure 12.

- The Weibull type models describe mineralising site growths (at all scales) in which the initial growth phase is long. After the initial growth phase, the period of time of the mineralising site development until death is very short. During this short growth time the maximum number of growth sites appears. Martyushev and Axelrod (2003) propose that these kinetics are associated with the shortest time for system development and maximum entropy production.

- The Fréchet type models represent mineralising site growths (at all scales) in which the initial growth phase is short. During this short growth time the maximum number of growth sites appears. The period of the mineralising site development to the death is highly variable, i.e., the mineralising growth can stabilize near reaching the maximum capacity or can take a long time to reach this value.

As we have indicated, for spatial distributions of mineralisation the Weibull fit is a direct arithmetic outcome of the fact that when one does a classical box count for point distributions then one is automatically carrying out a nearest neighbour analysis (as is proved implicitly in Blenkinsop and Sanderson, 1999). A nearest neighbour distribution is a special case of a Weibull distribution so it is inescapable that a Weibull distribution will result from a box-counting exercise; it does not necessarily have any physical significance. However some Weibull distributions (those with small γ) are close to a power-law as (it turns out) is the situation for the Agterberg data set.

What is of fundamental importance is the answer to the question: *What is the underlying statistical distribution that describes the spatial distribution of mineralised sites*? This is not obvious from the nearest neighbour analysis although such relations are considered by Sakhr and Nieminen (2018) and Carpena and Coronado (2019).

In order to understand what the spatial probability distribution might be one needs a relation between fracture or shear zone spacing and stress or some other parameter (assuming fractures and/or shear zones are the sites for mineralisation). Veveakis and Regenauer-Lieb (2015) and Alevizos et al. (2016) derive an expression for the spacing, h, of fractures and shear zones in a deforming fluid saturated material with a capped yield surface. The fractures result from stress singularities whose spacing is controlled by the fluid diffusivity; this means the fracture spacing is controlled by heterogeneities in the permeability in many instances. The argument is very general and includes opening/shear and compaction/shear bands as well as opening mode fractures both parallel and normal to (compressive) σ_1, together with pure compaction bands normal to σ_1. The overall behaviour of the system is governed by a dimensionless parameter, λ, defined as

$$\lambda = \frac{mechanical\ diffusivity}{fluid\ diffusivity} = \frac{\dot{\varepsilon}\mu_{fluid}}{kp'} L^2$$

where μ_{fluid} is the fluid viscosity, $\dot{\varepsilon}$ is the strain rate, p' is the mean stress and k is the permeability. L is the length of the system parallel to σ_1.

An informative view is to express the fracture spacing, h, in terms of λ (Alevizos et al. 2016, Figure 13):

$$h = \left(\frac{H}{0.26\sqrt{\lambda}} \right) = \sqrt{\frac{kp'}{\dot{\varepsilon}\mu_{fluid}}} \qquad (5)$$

Localisation of fractures does not occur until λ reaches a value of 13 (see Figure 13). This means that there is a lower cut off for λ, below which fractures do not occur. This is the type of behaviour for λ to be expected (Lavenda, 1965) of Weibull statistics and hence *h* (which is inversely proportional to $\lambda^{-1/2}$) is expected to have Fréchet statistics, This is identical to the classical distribution of fracture *lengths* derived from Weibull theory where the distribution of *stress* is Weibull but the distribution of fracture *lengths* is Fréchet (Lavenda, 1995, p180). The relation for Griffith cracks is $\sigma_y = \frac{C}{Y\sqrt{l}}$ where *C* is the fracture toughness, *Y* is a constant that depends on the crack shape and the stress/strain field and *l* is the fracture length. σ_y is the stress required to initiate fracture. There is a minimum stress below which fractures do not initiate. Thus the relation between σ_y and *l* for Griffith crack length is the same form as the relation between fracture spacing, *h*, and λ for generalised fracture development and the prediction is Fréchet distributions for crack length and crack spacing respectively.

We conclude that we expect the underlying statistical distribution for mineralised sites to be a Generalised Extreme Value distribution and its precise form depends on whether the distribution of λ is a Fréchet or a Weibull distribution. From (5) the distribution of mineralised sites is Fréchet if the distribution of strain rate is Weibull. The distribution of mineralised sites is Weibull if the distribution of permeability is Weibull. This conclusion is based on some physical arguments and is independent of the fact that the box counting algorithm always gives a nearest neighbour or Weibull distribution by definition. This is supported by the observed Fréchet and Weibull mass distributions from Zimbabwe. Further exploration of mineralising processes based on this approach may be found also in Ord and Hobbs (2021) and Ord et al. (2021).

4.2. Future work.

In order to establish the true spatial probability distributions for mineralised sites one approach is to employ *n*-point correlation functions (Kroner, 1971; Torquato, 2002; Kalidindi, 2015). Although such methods are widespread in the astronomy, materials and microstructure literature (and especially in the petroleum industry) we know of no applications in the characterisation of mineralisation. Such methods enable fractal or departures from fractal geometry to be quantified (Peebles, 1989, 1980; Jones et al., 2004) and should be pursued with vigour.

This paper has examined only data from orogenic gold deposits which (at least for vein-hosted deposits) we envisage as undergoing a nucleation-growth-death evolutionary history. For deposits where replacement processes or reaction-diffusion reactions dominate as in Pb-Zn deposits, or in gold deposits where gold/iron oxide replacement reactions or growth involving incorporation of gold in arseno-pyrite predominates, probability distributions other than GEV distributions are likely to be involved. These include Gamma and InverseGaussian distributions. Work in this regard is in progress.

5. Conclusions.

The spatial distributions of mineralisation (at least for the examples examined in this paper) are not fractal but belong to members of the Generalised Extreme Value (GEV) family of distributions. These members include the Weibull, Gumbel and Fréchet distributions. For some ranges of parameters some of these distributions can approximate scale invariant power-laws. The classical box counting method for spatial distributions of points is a method for calculating the nearest neighbour distribution which is a Weibull distribution. Hence all box counting methods produce a Weibull distribution; this may sometimes appear to be a bifractal but such an appearance does not have any physical significance. Many authors, having postulated a bifractal distribution, propose that different mechanisms must operate at small and large spatial scales. No physical explanation is given as to why this is so. The box counting procedure only gives a fractal dimension if the underlying distribution is a pure fractal. Otherwise the procedure gives a local fractal dimension which generally is spurious. Most examples examined here are best represented by Weibull distributions with a single Gumbel distribution. The underlying probability distribution is not a pure fractal. The best way of characterising the underlying probability distribution is to establish the mass distribution. For the examples examined this can be a Fréchet or Weibull distribution. Both these distributions are to be expected from current theories of fracture spacing. The cumulative distributions to be expected for spatial distributions are direct reflections of the growth kinetics of the mineralising system; nonlinear growth kinetics for nucleation-growth-extinction systems frequently lead to GEV probability distributions.

Acknowledgments.

We thank Jorn Kruhl and an anonymous reviewer for their useful comments.

References.

Agterberg, F. P. 2013**.** Fractals and spatial statistics of point patterns. Journal of Earth Science. 24, 001–011.

Agterberg, F. 2014. Geomathematics: Theoretical Foundations, Applications and Future Developments. Springer.

Alevizos, S., Poulet, T., Sari, M., Lesueur, M., Regenauer-Lieb. K., Veveakis. M. 2016. A framework for fracture network formation in overpressurised impermeable shale: deformability versus diagenesis. Rock Mech. Rock Eng. DOI 10.1007/s00603-016-0996-y.

Arneodo, A., Bacry, E., Muzy, J.F. 1995. The thermodynamics of fractals revisited with wavelets. Physica A 213, 232–275. (doi:10.1016/0378-4371(94)00163-N)

Bardi, U., Lavacchi, A., 2009. A simple interpretation of Hubbert's model of resource exploitation. Energies 2, 646–661.

Beck, C., Schlögl, F. 1995. Thermodynamics of chaotic systems. New York, NY: Cambridge Universit Press.

Blenkinsop, T. 2014. Scaling laws for the distribution of gold, geothermal, and gas resources. Pure Appl. Geophys. DOI 10.1007/s00024-014-0909-5

Blenkinsop, T. G. 1994. The fractal distribution of gold deposit: Two examples from the Zimbabwe Archean craton. In: Fractals and Dynamic Systems in Geoscience. Ed: J.

H. Kruhl. Springer. 247 – 258.

Blenkinsop, T. G. 1995. Fractal Measures for Size and Spatial Distributions of Gold Mines: Economic Implications. In: Blenkinsop, T. G., Tromp, P. L., eds., Sub-Saharan Economic Geology. Special Publication Geological Society of Zimbabwe, 3: 177–186.

Blenkinsop, T. G., and Sanderson, D. J. 1999. Are gold deposits in the crust fractals? A study of gold mines in the Zimbabwean craton. In: McCaffrey, K. J. W., Lonergan, L. & Wilkinson, J. J. (eds) Fractures, Fluid Flow and Mineralization. Geological Society, London, Special Publications, 155, 141-151.

Bódai, T. 2016. Extreme value analysis in dynamical systems: Two case studies. Nonlinear and Stochastic Climate Dynamics, Editors: Christian Franzke, Terence O'Kane. Cambridge University Press.

Callen, H.B. 1960. Thermodynamics: An Introduction to the Physical Theories of Equilibrium Thermostatics and Irreversible Thermodynamics. John Wiley and Sons, New York.

Carlson, C. A. 1991. Spatial distribution of ore deposits. Geology. 19, 111 -114.

Carpena, P., Coronado, A. V. 2019. Connection of the nearest-neighbour spacing and the local box-counting dimension for discrete sets. Phys. Rev. E. 100, 022205.

Chandrasekar, S. 1943. Stochastic problems in physics and astronomy. Reviews of Modern Physics 15, 89 pp.

Corral, A., González, A. 2019. Power law size distributions in geoscience revisited. Earth and Space Science. 6, 673–697

Cressie, N. A. C. 1993. Statistics for Spatial Analysis. John Wiley.

Dekking, M. 2005. A Modern Introduction to Probability and Statistics. Springer.

Doutre, R. C. 2018. Multi-scale organisation and geological controls on large orogenic gold deposits. PhD thesis, University of Western Australia.

Doutre, R., Micklethwaite, S., Kovesi, P., McCuaig, C. T., Ford, A., Hayward, N. 2015. Multi-scale spacing and endowment of orogenic gold deposits. Mineral Resources in a Sustainable world. 13th SGA Biennial Meeting Proceedings. 1, 81 – 84.

Fama, E. F. 1963. Mandelbrot and the stable Paretian hypothesis. The Journal of Business. 36, 420 – 429.

Fama, E. F. 1965. The behavior of stock-market prices. The Journal of Business. 38, 34-105.

Frank, S. A. 2009. The common patterns of Nature. J Evol. Biol. 22, 1563 – 1585.

Frank, S. A. 2019. The common patterns of abundance: the log series and Zipf's law. F1000Research, 8, 334.

Gibbs, J.W. 1875–1878. On the equilibrium of heterogeneous substances. Trans. Conn. Acad. Arts Sci. 3, 108–248 ((1875–6); 343–524 (7–8)).

Gnedenko, B.V., Kolmogorov, A.N. 1968. Limit distributions for sums of independent random variables (Translated from the Russian, annotated, and revised by K.L.

Chung with appendices by J.L. Doob and P.L. Hsu). Addison-Wesley, Reading.

Gumbel, E. J. 1954. Statistical theory of extreme values and some practical applications. Applied Mathematics Series, 33, Washington, D.C.: National Bureau of Standards, February 12, 1954.

Hobbs, B. E., Ord, A. 2021. Orogenic gold systems as nonlinear systems: Nonlinear analysis of data. In preparation.

Hobbs, B.E. ,Ord, A. 2018. Episodic modes of operation in hydrothermal gold systems: Part II. A model for gold deposition. Geological Society, London, Special Publications, 453, https://doi.ord/10.1144.SP453.15

Hodkiewicz, P. F., Weinberg, R. F., Gardoll, S. J., Groves, D. I. 2005. Complexity gradients in the Yilgarn Craton: fundamental controls on crustal-scale fluid flow and the formation of world-class orogenic-gold deposit. Australian Journal of Earth Sciences. 52, 831–841.

Hubbert, M.K., 1962. Energy Resources, National Academy of Sciences, National Research Council, Washington DC.

Jones, B, J. T., Martínez, V. J., Saar, E., Tribble, V. 2004. Scaling laws in the distribution of galaxies. Rev. Modern Physics. 76, 1211 – 1266.

Kalidindi, S. R. 2015. Hierarchical Materials Informatics. Elsevier.

Kroner, E. 1971. Statistical Continuum Mechanics. Courses and Lectures, 92, International Centre for Mechanical Sciences, Udine. Springer.

Kruhl, J. 2013. Fractal-geometry techniques in the quantification of complex rock structures: A special view on scaling regimes, inhomogeneity and anisotropy. Journal of Structural Geology 46, 2-21.

Lavenda, B. H. 1995. Thermodynamics of Extremes. Albion Publishing.

Lavenda, B. H., Florio, A. 1992. Thermodynamics of rare events. International Journal of Theoretical Physics. 31, 1445 – 1475.

Lucarini, V., Faranda, D., de Freitas, A. C. G. M. M., de Freitas, J. M. M., Holland, M., Kuna, T., Nicol, M., Todd, M., Vaienti, S. 2016. Extremes and Recurrence in Dynamical Systems. Wiley.

Mandelbrot, B. 1965. The statistics of natural resources and the law of Pareto. Chapter 1 In: Fractals in Petroleum and Earth Processes. Eds: CC. Barton, PR Pointe. Pleneum Press.

Mandelbrot, B. 1963. New methods in statistical economics. The Journal of Political Economy. 71, 421– 440.

Mandelbrot, B. 1960. The Pareto–Lévy Law and the distribution of income, International Economic Review. https://www.jstor.org/stable/2525289.

Mandelbrot, B. 1961. Stable Paretian random functions and the multiplicative variation of income. Econometrica. https://www.jstor.org/stable/pdfplus/1911802.pdf.

Mandelbrot, B. 1956. On the language of taxonomy: An outline of a “thermostatistical” theory of systems of categories with Willis (natural) structure. In; Information Theory: The third London symposium, Ed. C. Cherry, 135 – 145, Academic Press.

Martyushev, L.M., Axelrod, E.G. 2003. From dendrites and S-shaped growth curves to the maximum entropy production principle. JETP Letters. 78, 476-479.

Marwan, N., Roman, M.C., Thiel, M., Kurths, J. 2007. Recurrence plots for the analysis of complex systems. Phys. Rep. 438, 237–329. (doi:10.1016/j.physrep.2006.11.001)

Moller, J., Toftaker, H. 2014. Geometric anisotropic spatial point pattern analysis and Cox processes. Scandinavian Journal of Statistics. 41, 414 – 435.

Munro, M.A., Ord, A., Hobbs, B.E. 2018. Spatial organization of gold and alteration mineralogy in hydrothermal systems: wavelet analysis of drillcore from Sunrise Dam Gold Mine, Western Australia. In Characterization of ore-forming systems from geological, geochemical and geophysical studies. Geological Society, London, Special Publications, vol. 453 (eds K Gessner, TG Blenkinsop, P Sorjonen-Ward). London, UK: Geological Society. (doi:10.1144/ SP453.10).

Nair, J., Wierman, A., Zwart, B. 2021. The Fundamentals of Heavy Tails: Properties, Emergence, and Estimation. Unpublished but available at: https://adamwierman.com/book/. To be published by Cambridge University Press.

Ord, A., Hobbs, B. E. 2021. Orogenic gold deposits as nonlinear systems. Nonlinear analysis of data. Under revision. Ore Geology Reviews.

Ord, A., Blenkinsop, T. G., Hobbs, B. E. 2021. Fragment size distributions in brittle deformed rocks. Under revision. Journal of Structural Geology.

Ord, A., Hobbs, B., Dering, G., Gessner, K. 2018. Nonlinear analysis of natural folds using wavelet transforms and recurrence plots. Phil. Trans. R. Soc. A 376: 20170257.

Ord, A., Munro, M., Hobbs, B.E. 2016 Hydrothermal mineralising systems as chemical reactors: wavelet analysis, multifractals and correlations. Ore Geol. Rev. 79, 155–179. (doi:10.1016/j.oregeorev.2016.03.026)

Ord, A., Hobbs, B. E., Lester, D. R. 2012. The mechanics of hydrothermal systems: I. Ore systems as chemical reactors. Ore Geology Reviews. 49, 1 - 44.

Peebles, P. J. E. 1989. The fractal galaxy distribution. Physica D. 38, 273-278.

Peebles, P. J. E. 1980. The Large Scale Structure of the Universe. Princeton University Press.

Raines, G. L. 2008. Are fractal dimensions of the spatial distribution of mineral deposits meaningful ? Natural Resources Research, 17(2): 87–97.

Rocha, J. L., Aleixo, S. M. 2013. An extension of Gompertzian growth dynamics; Weibull and Fréchet models. Mathematical Biosciences and Engineering. 10, 379 – 398.

Sakhr, J., Nieminen, J. M. 2018. Local box-counting dimensions of discrete quantum eigenvalue spectra: Analytical connection to quantum spectral statistics. Phys Rev E.97, 030202.

Savageau, M. A. 1979. Growth of complex systems can be related to the properties of their underlying determinants. Proc. Nat. Acad. Sci. USA. 76, 5413-5417.

Savageau, M. A. 1980. Growth equations: A general equation and a survey of special cases. Mathematical Biosciences. 48, 267 -278.

Sethna, J. P. 2006. Statistical Mechanics: Entropy, Order Parameters, and Complexity. Oxford University Press.

Singer, D. A. 2013. The lognormal distribution of metal resources in mineral deposits. Ore Geology Reviews, 55, 80 - 86.

Singer, D. A., Menzie, W. D. 2010. Quantitative Mineral Resource Assessments. An Integrated Approach. Oxford University Press.

Sprott, J. C. 2003. Chaos and Time Series Analysis. Oxford.

Tippet, L. H. C. 1925. On the extreme individuals and the range of samples taken from a normal population. Biometrika, XVII, 364-87.

Torquato, S. 2002. Random Heterogeneous Materials. Springer.

Veveakis, E., Regenauer-Lieb, K. 2015. Cnoidal waves in solids. Journal of the Mechanics and Physics of Solids.78, 231 -248.

Wolfram Research, Inc., 2020. Mathematica, Version 12.2, Champaign, IL http://reference.wolfram.com/language/guide/ParametricStatisticalDistributions.html

Figure Captions

Figure 1. Classification of the heavy tailed distributions of interest. The regularly varying distributions are those that behave close to power laws as the population size increases. For details of this diagram and of the distributions within it see Nair et al. (2021). The γ quoted for the Weibull distribution in Appendix 2 is the extreme value index of (A4.1) in Appendix 4 and Figure A4.1.

Figure 2. The nearest neighbour density distribution, (2), as a log-log plot with n = 1000 and a square sample area 1000 km across. This is a Weibull density distribution with γ in (A4.1) equal to 0.5. The two red lines are attempts to define two linear regions with different “fractal dimensions”.

Figure 3. Analysis of data from Figure 4 of Agterberg (2013). (a) Reproduction of Figure 4 from Agterberg (2013) with his box count fit of D_{box} = 1.528 shown. (b) The data of Figure 4 shown on a linear-linear plot with a power law fit, $N(\varepsilon) = 309.2\ \varepsilon^{-1.206}$ shown. (c) Figure 4 of Agterberg (2013) reproduced showing that the data define a continuous parabolic curve. (d) D_{box} calculated from (c) using (4). (e) Weibull2 fit to data of Figure 4 using Mathematica

(Wolfram Research 2020). (f) Probability plot showing departures of data of Agterberg's Figure 4 from the Weibull2 fit. Weibull2 implies a two parameter Weibull distribution.

Figure 4. Mathematica (Wolfram Research 2020) fits to Agterberg data. (a) Single Pareto Type II fit. (b) Probability plot for single Pareto Type II fit.

Figure 5. Gamma distribution fit to Agterberg (2013, his Figure 4) data. Mathematica (Wolfram Research 2020) identifies this as a slightly better fit to the data than Weibull2.

Figure 6. Reproduction of Figure 7 from Blenkinsop and Sanderson (1999).

Figure 7. Best fit distributions for the data sets shown in Figure 6. (a and b) Craton; Weibull. (c and d) Bulawayo; Weibull. (e and f) Harare; Weibull. (g and h) Mashava; Weibull. (i and j) Shamva; Weibull. (k and l) Shamva; Gumbel). The location and relevant distribution is shown on each figure. For each location the probability distribution is shown followed by the probability plot which shows how good the fit is. The plots for Shamva data (i, j, k, l) show that a Gumbel distribution is a better fit than a Weibull distribution. The probability plots have *data* as the horizontal axis and *modelled* as the vertical axis.

Figure 8. Reproduction of Figure 7 from Blenkinsop (2014).

Figure 9. Best fit probability distribution for green data (crosses) in Figure 10. (a and b) Craton+production. This is a Fréchet3 distribution although there is departure from Fréchet3 at high mass values, The probability distribution for the red data (triangles; Craton, no production) in Figure 10 is almost identical to the distribution shown here for the green data. Fréchet3 implies a three parameter Fréchet distribution.

Figure 10. Best fit probability distribution for data from the Masvingo area (the black, straight line, data in Figure 8). This is a Weibull2 distribution with some departure at low mass levels.

Figure 11. A crustal scale mineral system where energy and mass are added from the lower crust or mantle. Some sites are places of energy dissipation and others are not. We identify the dissipation sites with mineralised sites. We want to know the spatial distribution of these energy dissipation sites. After Blenkinsop (2014).

Figure 12. Normalised sigmoidal curves: Weibull (blue), Gompertz (green) and Fréchet (red) with $\alpha = b$ = 1.3, 1.5, 1.9, 2, 4, 6. The normalised Weibull curves are for $f_N(t) = \exp(-(-t)^{\alpha})$ and have inflection points (black dots) for $f_N(t) > \frac{1}{e}$. The inflection point measures the number of mineralising sites developed at the peak of growth rate. The normalised Gompertz curves are for $f_N(t) = \exp(-\exp(-bt))$ and there is just one inflection point for the family at

$f_N(t) = \frac{1}{e}$. The normalised Fréchet curves are for $f_N(t) = \exp(-t^{-\alpha})$ and have inflection points for $f_N(t) < \frac{1}{e}$. From Rocha and Aleixo (2013).

Figure 13. Plots of localised effective stress against normalised distance, ξ / L, for various values of λ. Below $\lambda = 13$ no localisation occurs so there is a lower limit for λ where fractures do not form suggesting Weibull statistics for *l*. For $\lambda \geq 13$, the spacing follows the relation $h = L / \left(0.26\sqrt{\lambda}\right)$. Weibull statistics for λ results in Fréchet statistics for the spacing.

Appendix A1. Some background

Mandelbrot (1997) credits Fréchet (1941) with the first observation that the spatial distribution of some natural features follows the hyperbolic relation, (1). Mandelbrot realised that many natural phenomena are characterised by statistical distributions where the variance is infinite. To represent such phenomena he emphasised the power-law or Pareto distribution which became identified with the concept of fractals; the Pareto distribution has infinite mean and variance and has a fat tail so that it can represent extreme events. However he was aware of other fat tailed distributions such as those arising from Lévy stochastic processes (Mandelbrot, 1963). Even though the stable extreme distributions had been identified many years earlier (Fisher and Tippett, 1928; Gnedenko, 1943; Gnedenko and Kolmogorov, 1949 1968; 1949 in Russian), Mandelbrot did not use these distributions and his excursions into the statistics of extremes ended with some Lévy distributions capable of accommodating skewness and the sub-exponential decaying tails of observed distributions, in contrast to the thin and rapidly decaying tails of the normal distribution.

Authors in the geological literature became infatuated with the concept of fractals, encouraged by the book by Mandelbrot (1982) and influential works by Mandelbrot (1965), Barton and Scholtz (1965), La Pointe (1995) and Turcotte (1986, 1989). The result is that the Pareto distribution has become the heavy tailed distribution of choice in the geological literature especially if the distribution is power-law like in appearance. Moreover, the concepts of nonlinear behaviour, critical behaviour and fractal geometry have become widely inter-linked with the implication that any nonlinear behaviour automatically leads to power-law probability distributions for variants produced by such behaviour. This is especially emphasised in the notion that fractal geometries and power-law distributions arise from self-organised criticality (Hronsky and Groves, 2008; McCuaig and Hronsky, 2014). This association of Pareto distributions with nonlinear systems has not proved correct and the literature on GEV distributions arising from nonlinear dynamical systems is now immense (see Lucarini et al., 2016 for examples). It is the Generalised Extreme Value family of probability functions that characterise nonlinear systems rather than Pareto distributions (Nicolis et al., 2006; Lucarini et al., 2012, 2014, 2016). In saying this one should also appreciate that the extremes of the GEV distributions are commonly (see Lucarini et al., 2016 as an example) represented by Generalised Pareto Distributions (GPD) which include the exponential distribution (as the tail of a Gumbel distribution) and the Pareto distribution (as the tail of a Fréchet distribution). A system at criticality (that is, a system that has evolved to be scale free) is by definition characterised by a Pareto distribution.

In summary, Mandelbrot (1963) and Fama (1965) proposed the Lévy stable distribution to represent skewed heavy tailed distributions as an alternative to the Gaussian distribution to characterise commodity and financial systems. Although there are many heavy-tailed (see Figure 1) alternatives to the Gaussian distribution (see Nair et al., 2021), the fundamental reason for selecting Lévy stable distributions is that they arise from the Generalized Central Limit Theorem, which states that stable laws are the only possible limit distributions for properly normalized and centred sums of independent, identically distributed random variables. An important further outcome of this theorem extended to distributions that lack a mean or variance is that there are just three extreme stable distributions that are members of the Generalised Extreme Value (GEV) distribution family. These are the Gumbel, Weibull and Fréchet distributions.

References A1

Barton. C. C., and Scholtz, C. H. 1965. The fractal size and spatial distribution of hydrocarbon accumulations. Chapter 2 In: Fractals in Petroleum and Earth Processes. Eds: CC. Barton, PR Pointe. Pleneum Press. 13 – 34.

Fama, E, F, 1965. The behavior of stock-market prices. The Journal of Business. 38, 34-105.

Fisher, R. A., Tippett, L. H. C. 1928. Limiting forms of the frequency distribution of the largest and smallest member of a sample. Proceedings of the Cambridge Philosophical Society, 24, 180–190.

Fréchet, M. 1941. Sur la loi de répartition de certaines grandeurs géographiques. J. Soc. Statistique de Paris. 82, 114 – 122.

Gnedenko, B. V. 1943. Sur la distribution limite du terme maximum d'une serie aleatoire. Annals of Mathematics, 44:423–453.

Gnedenko, B.V., Kolmogorov, A.N. 1968. Limit distributions for sums of independent random variables (Translated from the Russian, annotated, and revised by K.L. Chung with appendices by J.L. Doob and P.L. Hsu). Addison-Wesley, Reading.

Hronsky, J. N. A., Groves, D. I. 2008. Science of targeting: definition, strategies, targeting and performance measurement. Australian Journal of Earth Sciences, 55, 3-12.

La Pointe, P. R. 1995. Estimation of undiscovered hydrocarbon potential through fractal geometry. Chapter 3 In: Fractals in Petroleum and Earth Processes. Eds: CC. Barton, PR Pointe. Plenum Press. 35 – 57.

Lucarini, V., Faranda, D., de Freitas, A. C. G. M. M., de Freitas, J. M. M., Holland, M., Kuna, T., Nicol, M., Todd, M., Vaienti, S. 2016. Extremes and Recurrence in Dynamical Systems. Wiley.

Lucarini, V., Faranda, D., Wouters, J., Kuna, T. 2014. Towards a general theory of extremes for observables of chaotic dynamical systems. Journal of Statistical Physics, 154, 723–750.

Lucarini, V., Faranda, D., Turchetti, G., Vaienti, S. 2012. Extreme value theory for singular measures. Chaos, 22(2).

Mandelbrot, B. B. 1997. Fractals and Scaling in Finance. Springer.

Mandelbrot, B. B. 1982. The fractal geometry of nature. San Francisco, Freeman.

Mandelbrot, B. 1965. The statistics of natural resources and the law of Pareto. Chapter 1 In: Fractals in Petroleum and Earth Processes. Eds: CC. Barton, PR Pointe. Pleneum Press.

Mandelbrot, B. 1963. New methods in statistical economics. The Journal of Political Economy. 71, 421– 440.

McCuaig. T.C., Hronsky. J. M, A. 2014. The mineral system concept: the key to exploration targeting. Soc Econ Geol. Spec. Pub. 18, 153–175.

Nair, J., Wierman, A., Zwart, B. 2021. The Fundamentals of Heavy Tails: Properties, Emergence, and Estimation. Unpublished but available at: https://adamwierman.com/book/. To be published by Cambridge University Press.

Nicolis, C., Balakrishnan, V., Nicolis, G. 2006. Extreme events in deterministic dynamical systems. Physical Review Letters, 97:210602.

Turcotte, D. L. 1986. A fractal approach to the relationship between ore grade and tonnage. Econ. Geol. 81, 1528 – 1532.

Turcotte, D. L. 1989. Fractals in geology and geophysics. PAGEOPH. 131, 171 – 196.

Table A2.1. Some probability distributions pertinent to spatial distributions. In this table, α is the shape factor, β is the scale factor, μ is the position factor, m is the mean and σ^2 is the variance. <*a*> denotes the average of the quantity, *a*.

Distribution	Probability Distribution Function, *y* (*x*).	Physical significance	Maximum entropy constraints	Graphical density distributions
Generalised Extreme Value	$y=f(x;\alpha,\beta,\mu)=\frac{1}{\beta}t(x)^{\alpha+1}\exp(-t(x))$ $where\ t(x)=\left(1+\alpha\left(\frac{x-\mu}{\beta}\right)\right)^{-\frac{1}{\alpha}}\quad if\ \alpha\neq 0$ $=\exp\left(-\frac{x-\mu}{\beta}\right)\quad if\ \alpha=0$ **If $\alpha = 0$ this is a Gumbel distribution. If $\alpha > 0$ this is a Fréchet distribution. If $\alpha < 0$ this is a Weibull distribution.**	**A family of extreme value stable distributions. The Gumbel (Type I), Fréchet (Type II) and Weibull (Type III) as specific examples.**	**Types I, II and III arise from two constraints. One constraint sets the average location; the other is a measure of the average tail weighting.**	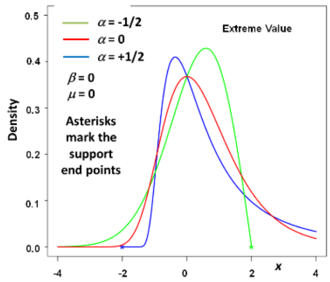
Gumbel	$y=f(x;\beta,\mu)=\frac{1}{\beta}\exp\left(-\left(z+\exp(-z)\right)\right)$ **where** $z=\frac{x-\mu}{\beta}$ **Tail of distribution is an exponential distribution**	**Corresponds to systems that nucleate, grow competitively and have moderate extinction times due to competition between processes.**	**To maximise entropy average location parameter is <*x*>. Average tail weighting is <exp(-*x*)>**	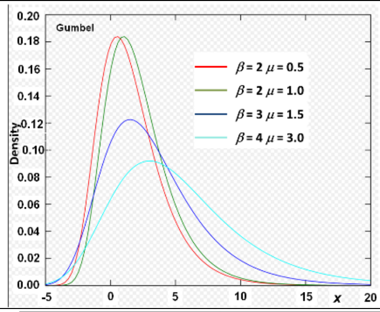
Fréchet	$y=f(x;\alpha,\beta,\mu)=\frac{\alpha}{\beta}(z)^{-1-\alpha}\exp(-(z))^{-\alpha}$ **where** $z=\frac{x-\mu}{\beta}$ **Tail of distribution is a power law distribution**	**Corresponds to systems that nucleate quickly, grow competitively and have long extinction times due to relatively weak competition.**	**To maximise entropy average location parameter is <log *x*>. Average tail weighting is <*x*$^{-\delta}$> where δ is the power law exponent for the tail**	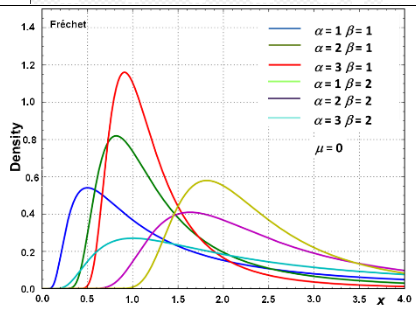
Weibull	$y=f(x;\alpha,\beta)=\frac{\alpha}{\beta}\left(\frac{x}{\alpha}\right)^{\beta-1}\exp\left(-\left(\frac{x}{\alpha}\right)^{\beta}\right);x\geq 0$ $=0;\ x<0$ **If *X* is Weibull then** $\sqrt{X}$ **is Exponential** $\left(\frac{1}{\sqrt{X}}\right)$ **If *X* is Weibull then** $\frac{1}{X^m}$ **is Fréchet**	**Corresponds to systems that nucleate quickly, grow competitively and have short extinction times due to relatively strong competition.**	**To maximise entropy average location parameter is <log *x*>. Average tail weighting is <(*M-x*)$^{\delta}$> where *M* is the maximum value of *x* and δ is the power law exponent for the truncated tail**	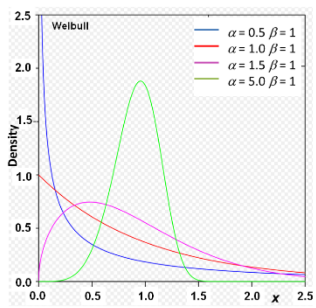

Pareto or power law	$y = f(x;\alpha,\mu) = \frac{\alpha\mu^{p}}{x^{p+1}}$	**A Pareto distribution often arises for the last few percentiles of a log normal distribution.**	**A special case of the log normal distribution for systems where the growth in the value of a variable in successive time intervals is proportional to the value of the variable in the previous time interval**	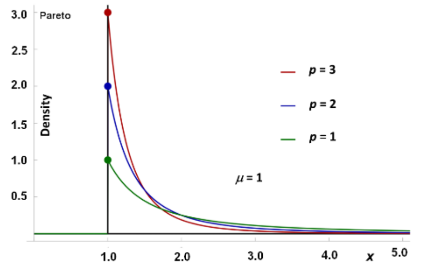
Log-normal	$y = f(x;e,\sigma) = \frac{1}{x\sigma\sqrt{2\pi}}\exp\left(-\left(\frac{(\ln x - e)^{2}}{2\sigma^{2}}\right)\right)$	**Closely related to GEV-distributions but can differ in detail. Those distributions arise from growth-competitive (birth-death) processes. Also can be coupled to diffusion processes (Crescenzo and Paraggio, 2019).**	**Maximises entropy for fixed geometric mean. If a system grows such that the growth in successive time intervals is a proportion of that in previous time interval the probability distribution is likely to be log normal.**	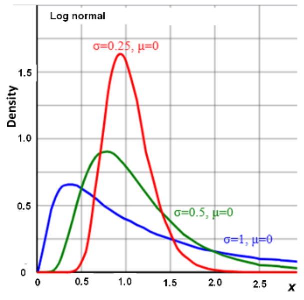
Normal	$y = f(x;e,\sigma^{2}) = \frac{1}{\sigma\sqrt{2\pi}}\exp\left(-\frac{1}{2}\left(\frac{x-e}{\sigma}\right)^{2}\right)$	**Typical of systems at equilibrium. If a system is controlled by processes that result in small variations from the mean then the probability distribution is likely to be normal.**	**Maximises entropy for fixed variance. Many distributions closely resemble normal distributions for some range of parameters as shown in above diagrams**	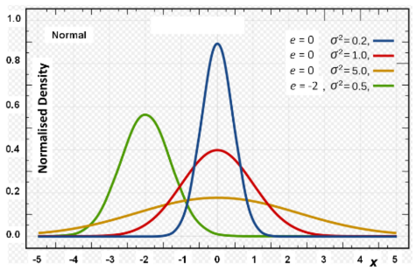

url's for figures in Table A2; last accessed 10 January 2022: https://en.wikipedia.org/wiki/ Fréchet_distribution ; https://en.wikipedia.org/wiki/Generalized_extreme_value_distribution ; https://en.wikipedia.org/wiki/Gumbel_distribution ; https://en.wikipedia.org/wiki/Log-normal_distribution ; https://en.wikipedia.org/wiki/Normal_distribution ; https://en.wikipedia.org/wiki/Pareto_distribution ; https://en.wikipedia.org/wiki/Weibull_distribution

References A2

Crescenzo, A. Di, Paraggio, P. 2019. Logistic growth described by birth-death and diffusion processes. Mathematics 7, 489. doi:10.3390/math7060489.

Appendix A3. Closed systems at equilibrium.

One of the simplest statistical distributions after the uniform distribution is the Gaussian distribution which results from stochastic processes operating with no correlation between events. The underlying thermodynamic constraint for this distribution is that differential entropy is maximized for a given variance. A Gaussian random variable has the largest entropy amongst all random variables of equal variance, or, alternatively, the maximum entropy distribution under constraints of mean and variance is the Gaussian. This distribution follows directly from the Law of Large Numbers (which states that for data with a well-defined mean and variance the mean of the distribution will approach that of the sample as the sample size increases) and the Central Limit Theorem which states that independent and identically distributed (i.i.d.) random variables with finite non-zero variances will tend to a Gaussian distribution as the number of variables grows. Thus the Gaussian distribution is precisely defined by the Central Limit Theorem with a mean specified by the Law of Large Numbers and a variance that maximises the differential entropy. It is a thin tailed distribution. The Gaussian distribution results from processes where there are strong physical, chemical or genetic controls that limit the variation around a mean value such as in the probability distribution for the heights of adult humans.

The log-normal distribution is defined in a similar manner to the Gaussian distribution; the Central Limit Theorem now applies to the logarithms of the variates rather than to the variates themselves. The log-normal distribution is the maximum entropy probability distribution for a random variate, X, for which both the mean and variance of ln(X) are specified. The log-normal distribution is fat tailed and so is used to model some fat tailed distributions. As indicated, since both the Gaussian and log-normal distributions maximise the entropy they are relevant to closed systems at equilibrium.

A distribution that defines the distribution or partitioning of energy in an isolated system is the classical Boltzmann distribution which proposes that the probability, p_i, that a given state, *i,* should have an energy, E_i, is given in terms of the fraction of states, $\frac{N_i}{N}$, that have an energy, E_i, as

$$p_i = \frac{N_i}{N} = \frac{\exp\left(-E_i / kT\right)}{Z} \qquad \text{(A3.1)}$$

where N_i is he number of states that have energy, E_i, N is the total number of states, k is Boltzmann's constant and T is the absolute temperature. Z (*the canonical partition function*) is present to ensure all accessible states add up to 1 and is given by

$$Z = \sum_{j-1}^{M} \exp\left(-E_j / kT\right) \qquad \text{(A3.2)}$$

The Boltzmann distribution, (A3.1), maximises the entropy of the system, $S = -\sum_{i=1}^{M} p_i \log p_i$, subject to the constraint that the mean energy of the system is $\sum p_i E_i$. The Boltzmann distribution is the basis of classical statistical thermodynamics and hence has particular relevance to the discussion of equilibrium states in isolated thermodynamic systems.

Of course there are many other distributions that maximise entropy for various constraints (Dawson and Wragg, 1973; Frank, 2009) but many are relevant to systems at equilibrium. The relevant distribution for a system at equilibrium depends on the scale of the distribution, the number of ways in which the events can occur, and the moments of the distribution (Lienhard and Myer, 1967).

For spatial systems at equilibrium, similar statements hold. For instance (McFadden, 1965) the point distribution that corresponds to maximum entropy for a given density is the Poisson distribution. As we have indicated, natural examples are commonly proposed to be the fractal random fields represented by a fractal dimension (Carlson, 1991; Blenkinsop, 1994, 1995, 2014; Hodkiewicz et al., 2005). Methods (other than box counting) of establishing the fractal dimension of random spatial fields with scale invariance are given by Biermé (2017).

References A3

Biermé, H. 2017. Introduction to random fields and scale invariance. Hal-01493834v2. https://hal.archives-ouvertes.fr/hal-01493834v2.

Blenkinsop, T. G., 1994. The fractal distribution of gold deposit: Two examples from the Zimbabwe Archean craton. In: Fractals and Dynamic Systems in Geoscience. Ed: J. H. Krühl. Springer. 247 – 258.

Blenkinsop, T. G., 1995. Fractal Measures for Size and Spatial Distributions of Gold Mines: Economic Implications. In: Blenkinsop, T. G., Tromp, P. L., eds., Sub-Saharan Economic Geology. Special Publication Geological Society of Zimbabwe, 3: 177–186.

Blenkinsop, T. 2014, Scaling laws for the distribution of gold, geothermal, and gas resources. Pure Appl. Geophys. DOI 10.1007/s00024-014-0909-5

Carlson, C. A. 1991. Spatial distribution of ore deposits. Geology. 19, 111 -114.

Dawson, D. C., Wragg, A. 1973. Maximum-entropy distributions having prescribed first and second moments. IEEE Trans. Info. Theory, 19, 689 – 693.

Frank, S, A. 2009. The common patterns of Nature. J Evol. Biol. 22, 1563 – 1585.

Hodkiewicz, P. F., Weinberg, R. F., Gardoll, S. J., Groves, D. I. 2005. Complexity gradients in the Yilgarn Craton: fundamental controls on crustal-scale fluid flow and the formation of world-class orogenic-gold deposit. Australian Journal of Earth Sciences. 52, 831–841.

Lienhard, J. H., Myer, P. L. 1967. A physical basis for the generalised gamma distribution. Quart. Appl. Math.25, 330 – 334.

McFadden, J.A. 1965. The mixed Poisson process. Sankhya: The Indian Journal of Statistics A, 27, 83-92.

Appendix A4. Open systems far from equilibrium.

A generalisation of the Central Limit Theorem by Gnedenko and Kolmogorov (1968) states that the sum of a number of random variables with symmetric distributions having infinite variance, will tend to a *stable* distribution as the population increases. The family of distributions corresponding to this limit are the *Generalised Extreme Value* (GEV) distributions. The important concept here is that the extreme values of an initial distribution (namely, those in the tail of the initial distribution, Figure A4.2a) have their own probability distributions known as extreme value distributions. The initial distributions for relatively small populations are asymptotic to the extreme distributions as the population increases. These asymptotic distributions are said to be *attractors* for the initial distribution. The only stable distributions that correspond to the tails of other distributions (those that belong to the family of generalised extreme value (GEV) distributions) and that have a formal mathematical expression are the *Weibull*, *Gumbel* and *Fréchet* distributions (Figure A4.1).

The generalised extreme value distributions are given by

$$H(x) = \exp\left[-\left(1 + \gamma\left(\frac{x-\mu}{\varphi}\right)\right)_{+}^{-1/\gamma} \right] \quad \text{(A4.1)}$$

The family of extreme value distributions (EVD) is given by

$$H_{\gamma}(x) = \exp\left[-(1+\gamma x)_{+}^{-1/\gamma} \right] \text{ if } \gamma \neq 0 \quad \text{(A4.2)}$$

[2]

$$H_{\gamma}(x) = \exp\left[-\exp^{-x} \right] \text{ if } \gamma = 0 \quad \text{(A4.3)}$$

where $H_{\gamma}(x)$ is the cumulative distribution function of the Extreme Value Distribution of the random variable, *x*, with $\gamma = \frac{1}{\alpha}$ the *extreme-value index*. For a detailed discussion of these distributions see Nair et al. (2021).

[2] The symbol $(y)_{+}$ means that the quantity inside the brackets takes the maximum value between 0 and *y*.

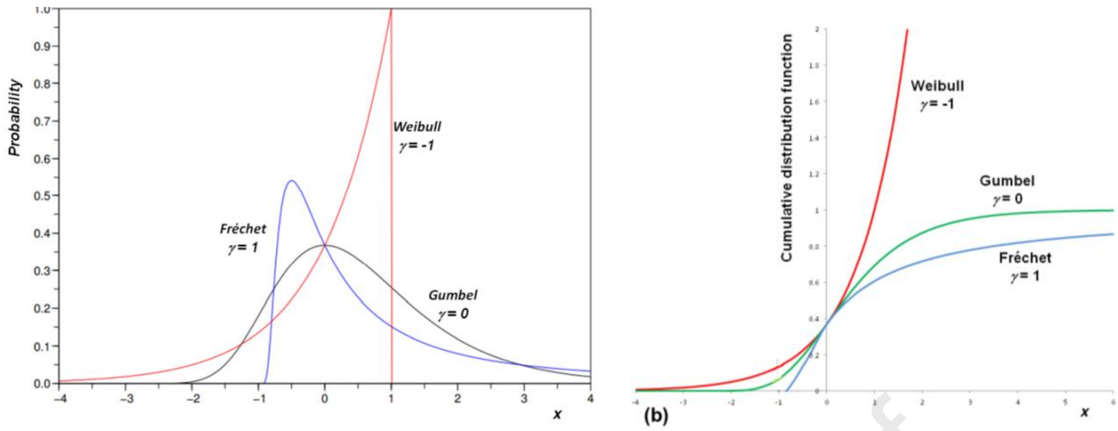

Figure A4.1. Probability distributions for members of the extreme value distributions with values of the extreme value index, γ, indicated. (a) Density distribution functions. (b) Cumulative distribution functions.

Depending on the sign of γ, three maximum domains of attraction are defined (Figure A4.1):

If $\gamma > 0$, $H(x)$ belongs to the Fréchet maximum domain of attraction. This domain of attraction includes distributions with *heavy* tails, i.e. their initial distribution functions decrease as a power function or more slowly.

If $\gamma = 0$, $H(x)$ belongs to the Gumbel maximum domain of attraction. This domain of attraction includes distributions with *light* tails, i.e. their initial distribution functions decrease as an exponential function.

If $\gamma < 0$, $H(x)$ belongs to the Weibull maximum domain of attraction. This domain of attraction includes distributions with *short* tails, i.e. they have a finite endpoint. Although the Weibull distribution is short tailed it can be either heavy-tailed or light-tailed.

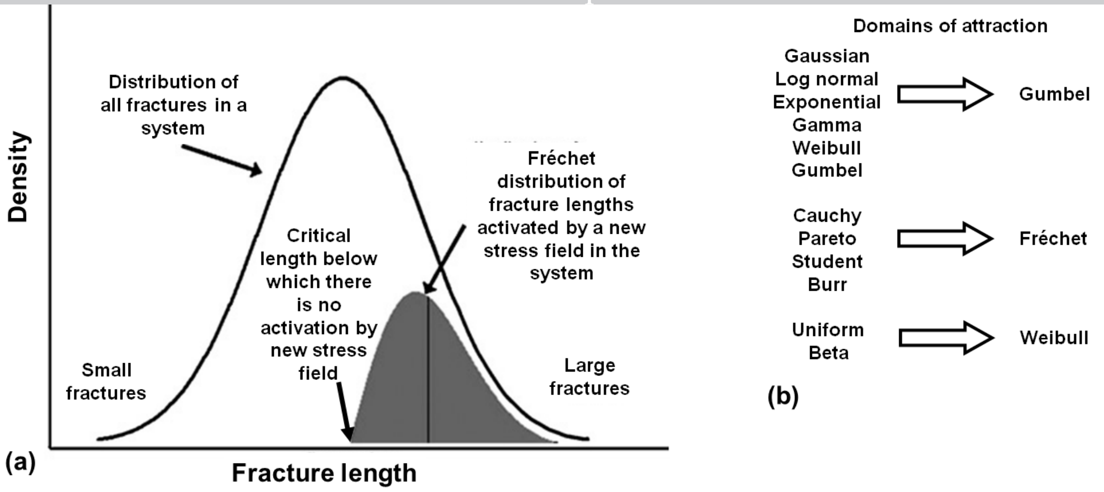

Figure A4.2 . Asymptotic distributions. (a) An initial distribution shown as the full line. This could for instance represent the probability distribution of all fractures in an area. The distribution of fractures activated by a new stress field is shown in gray. Griffith theory predicts there is a critical length below which reactivation does not occur. The probability distribution of activated fracture is Fréchet (although the distribution of stress sites is Weibull; Lavenda, 1995, p180). In this case the Fréchet distribution is the domain of attraction of the initial distribution. (b) Common initial distributions and their domains of attraction. After Embrechts et al. (1997, Chapter 3) and Quinn and Quinn (2010).

The following relations exist between the three stable extreme distributions:

If X has a Fréchet distribution (commonly written Φ_α), then -1/X has the Weibull distribution (commonly written Ψ_α) and log(X^α) has a Gumbel distribution (commonly written, Λ_α).

Lavenda (1995, pp 6, 78 - 79) presents a thermodynamic explanation for the stable distributions. For a closed system the entropy must always increase as the system evolves to maximum entropy at equilibrium. However an open system can exchange entropy with its environment. So that although the total entropy, S, of the system plus its environment must always increase towards equilibrium to satisfy the second law of thermodynamics, the internal entropy can decrease as long as the decrease in internal entropy, $\Delta S_{internal}$, is compensated by an increase in entropy of the environment, $\Delta S_{external}$. Thus the generation of ordered structures and patterns in systems far from equilibrium is associated with an internal entropy reduction, $\Delta S_{internal}$ (Kondepudi and Prigogine, 1998).

Lavenda shows that

$$\Delta S_{internal}(x) = -(1-\alpha)\left(\frac{\beta}{x}\right)^{\frac{\alpha}{1-\alpha}}$$

where α is a constant $0 < \alpha < 1$. This has the form of a Fréchet distribution:

$$\Delta S_{internal}(x) = \ln G(x) = -cx^{-D}$$

The Fréchet distribution can be considered as the generalisation for extreme value distributions of the Boltzmann principle (Lavenda , 1995, pp 6, 49-51, 149; Lavenda and Florio, 1992). Hence in an open system far from equilibrium we expect the energy to be partitioned so as to follow a Fréchet distribution just as in a closed system at equilibrium the equipartition of energy follows a Boltzmann distribution as discussed in Appendix A3.

For a Weibull distribution Lavenda (1995, pp79) shows that

$$\Delta S_{internal}(x) = -(\alpha - 1)\left(\frac{x}{\beta}\right)^{\frac{\alpha}{\alpha-1}}$$

References A4

Embrechts, P., Klüppelberg, C., Mikosch, T. 1997. Modelling Extreme Events for Insurance and Finance. Springer.

Gnedenko, B.V., Kolmogorov, A.N. 1968. Limit distributions for sums of independent random variables (Translated from the Russian, annotated, and revised by K.L. Chung with appendices by J.L. Doob and P.L. Hsu). Addison-Wesley, Reading.

Kondepudi,D., Prigogine, I. 1998. Modern Thermodynamics, Wiley.

Lavenda, B. H. 1995. Thermodynamics of Extremes. Albion Publishing.

Lavenda, B. H., Florio, A. 1992. Thermodynamics of rare events. International Journal of Theoretical Physics. 31, 1445 – 1475.

Nair, J., Wierman, A., Zwart, B. 2021. The Fundamentals of Heavy Tails: Properties, Emergence, and Estimation. Unpublished but available at: https://adamwierman.com/book/. To be published by Cambridge University Press.

Quinn, J. B., Quinn, G. D. 2010. A practical and systematic review of Weibull statistics for reporting strengths of dental materials. Dental Materials. 26, 135–147.

Table 1. Ranking of probability distribution fits for Agterberg data.

Gamma	0.92
Weibull2[2]	0.89
Log-normal	0.76
Weibull 3	0.49
Pareto 3	0.49
Fréchet 3	0.49
Fréchet 2	0.43
Inverse Gaussian	0.40
Gumbel	0.20

[2] Weibull2, Weibull3 refer to two and three parameter distributions respectively. A 2-parameter representation involves only the scale and shape factors in Table 1; the 3-parameter representation involves the position factor in addition. The same notation applies to the other distributions.

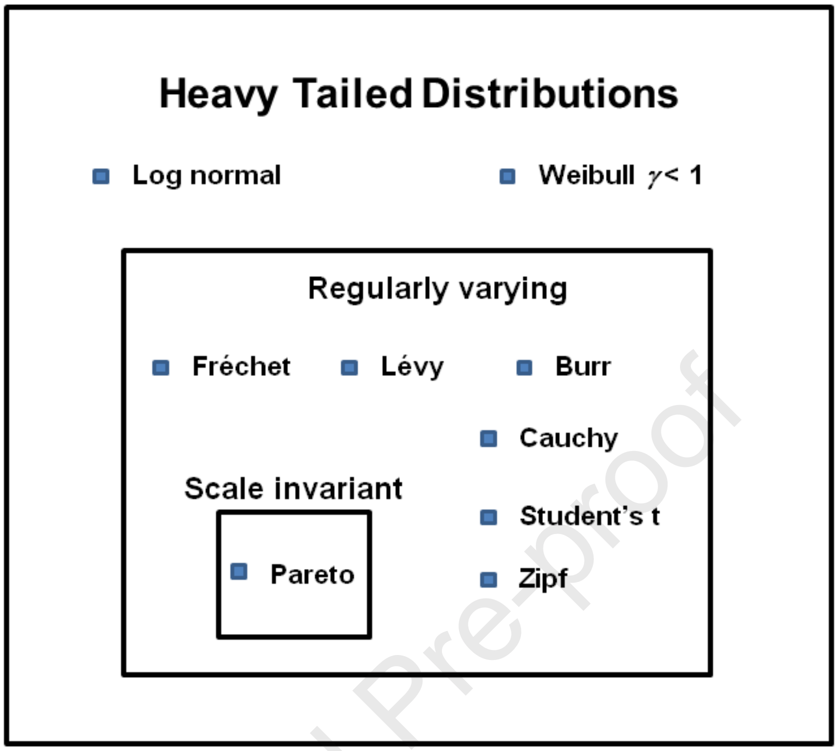
Heavy Tailed Distributions
Log normal
Weibull γ< 1
Regularly varying
Fréchet
Lévy
Burr
Cauchy
Scale invariant
Student's t
Pareto
Zipf

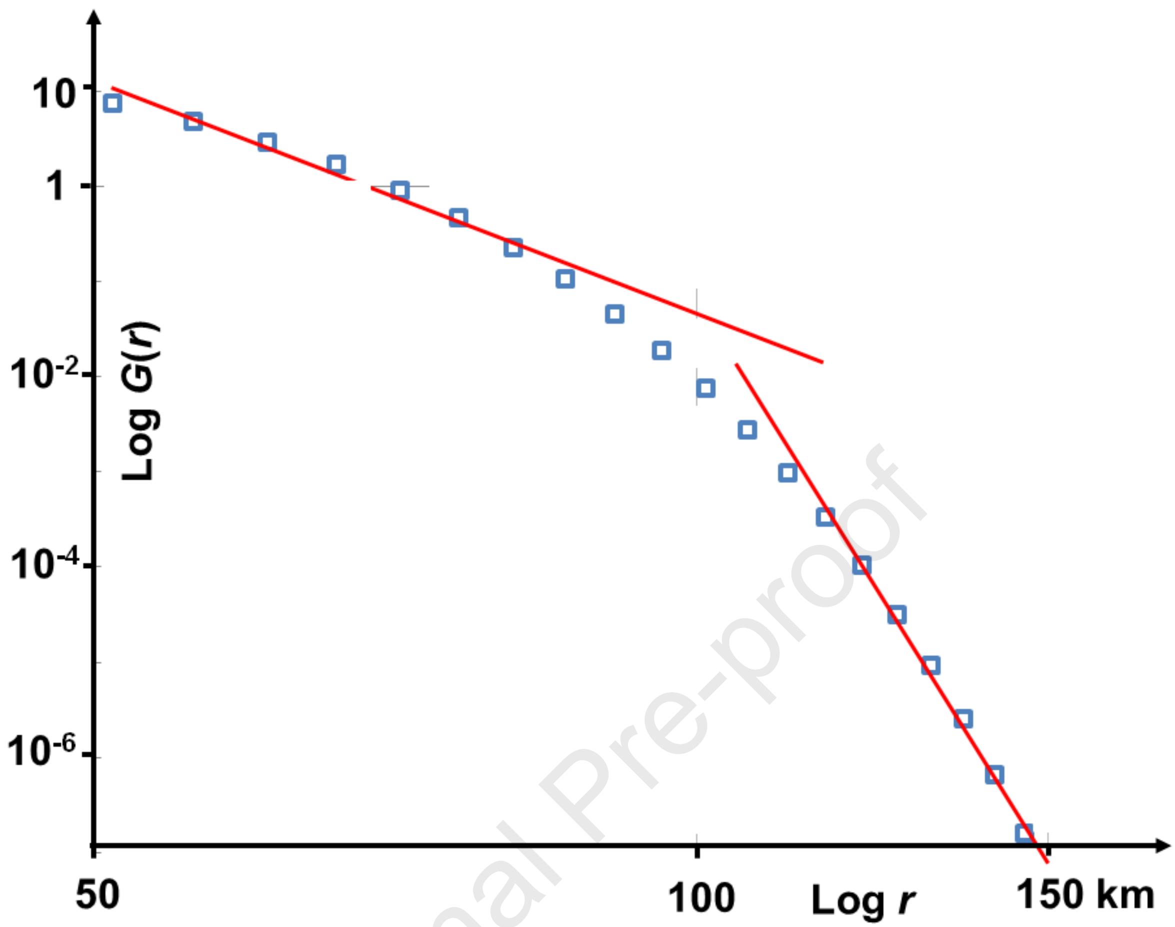
10
1
10-2
10-4
10-6
Log G(r)
50
100
Log r
150 km

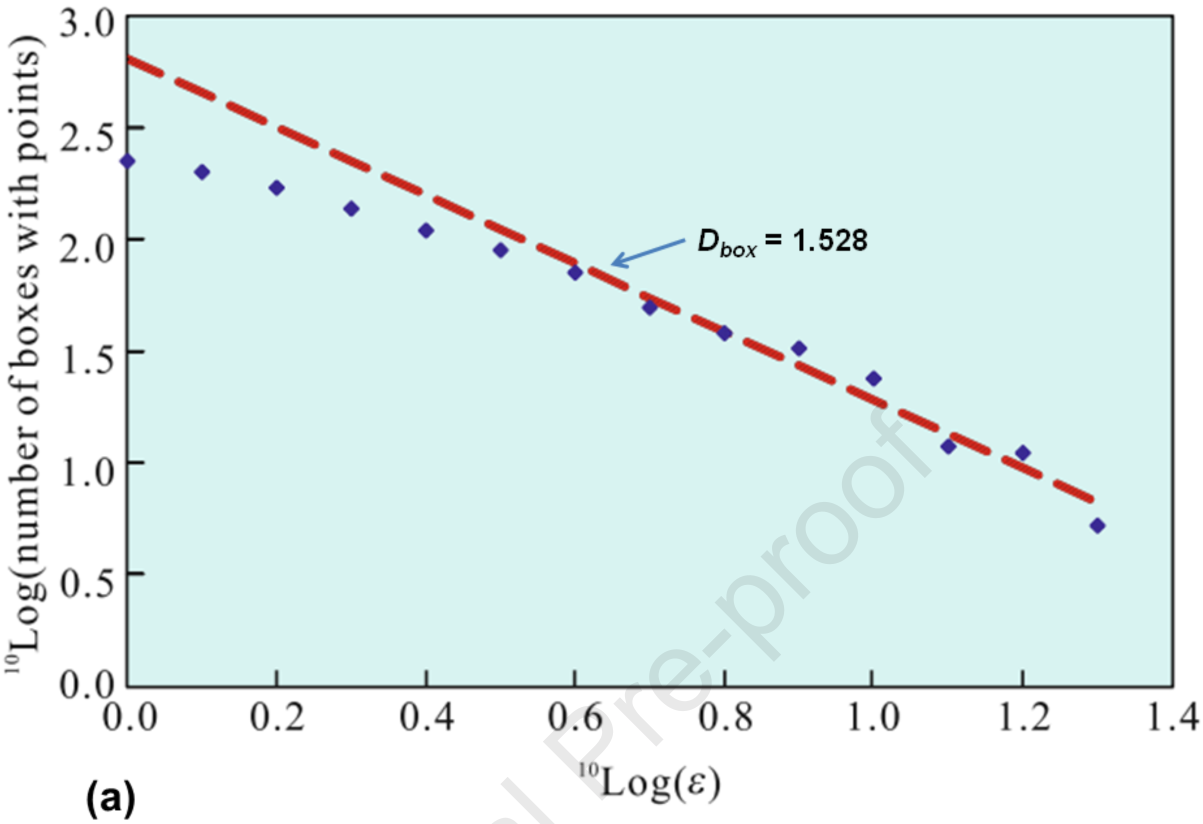

3.0
2.5
2.0
1.5
1.0
0.5
0.0
0.0
0.2
0.4
0.6
0.8
1.0
1.2
1.4
^{10}Log(number of boxes with points)
^{10}Log(ε)
D_{box} = 1.528

(a)

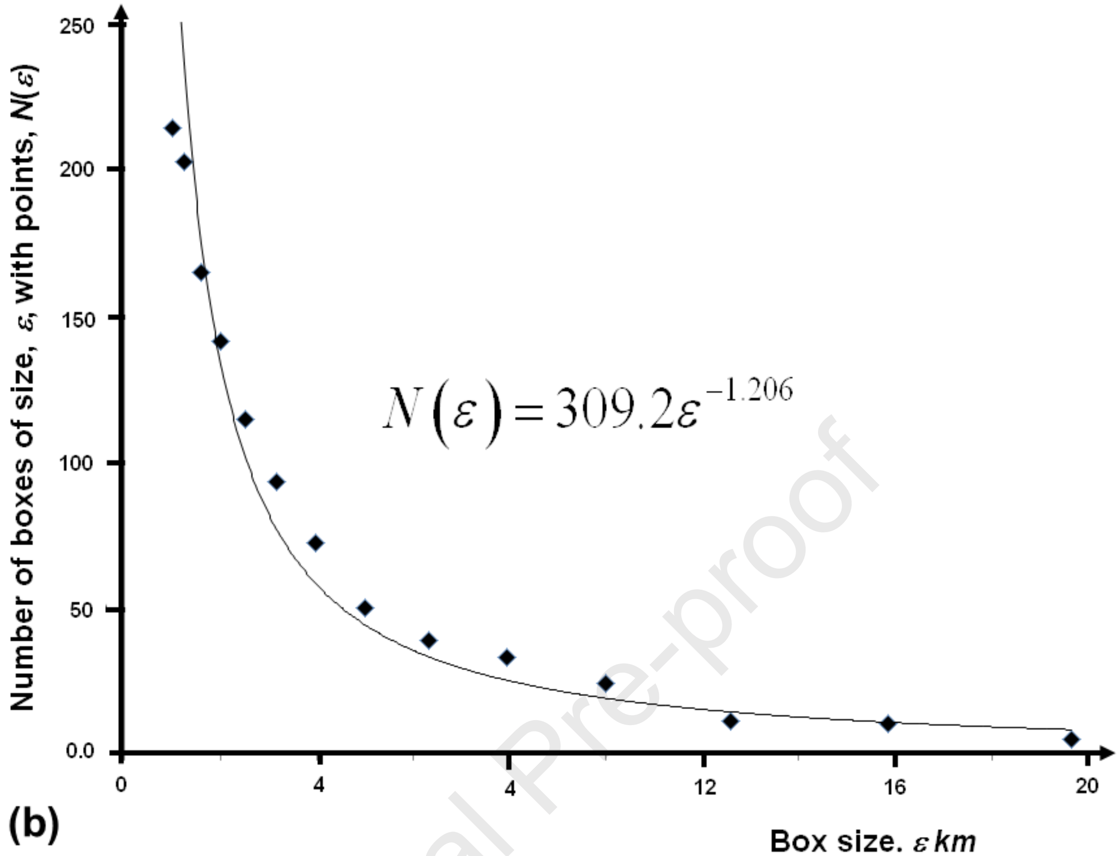
250
200
150
100
50
0.0
Number of boxes of size, ε, with points, N(ε)
$N(\varepsilon) = 309.2\varepsilon^{-1.206}$
0
4
4
4
12
16
20
Box size. ε km

(b)

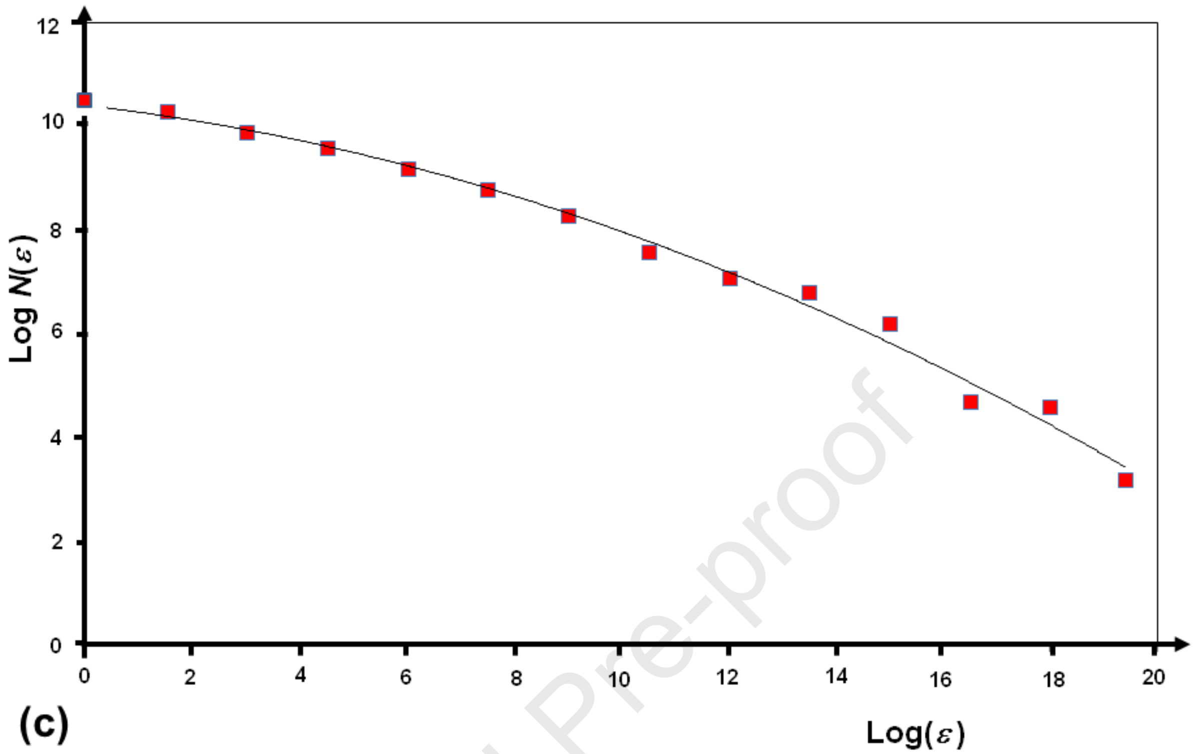
12
10
8
6
4
2
0
Log $N(\varepsilon)$
0
2
4
6
8
10
12
14
16
18
20
Log(ε)

(c)

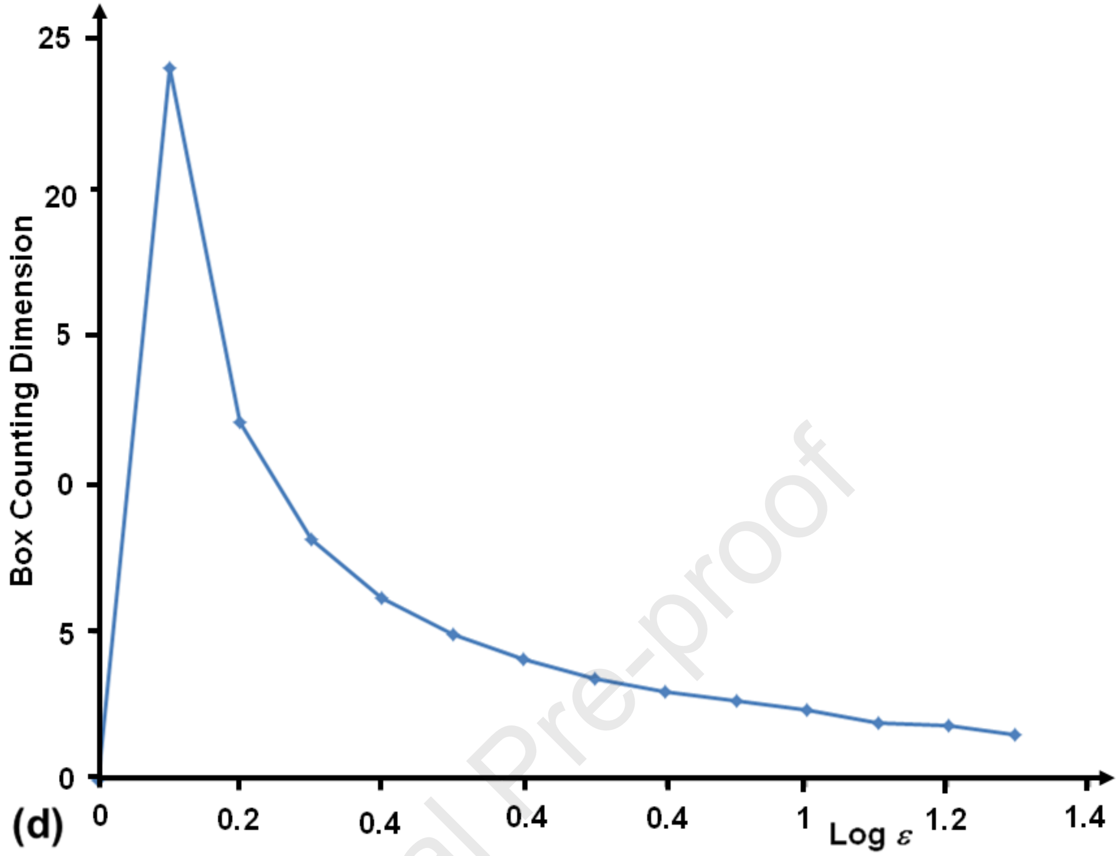

(d)

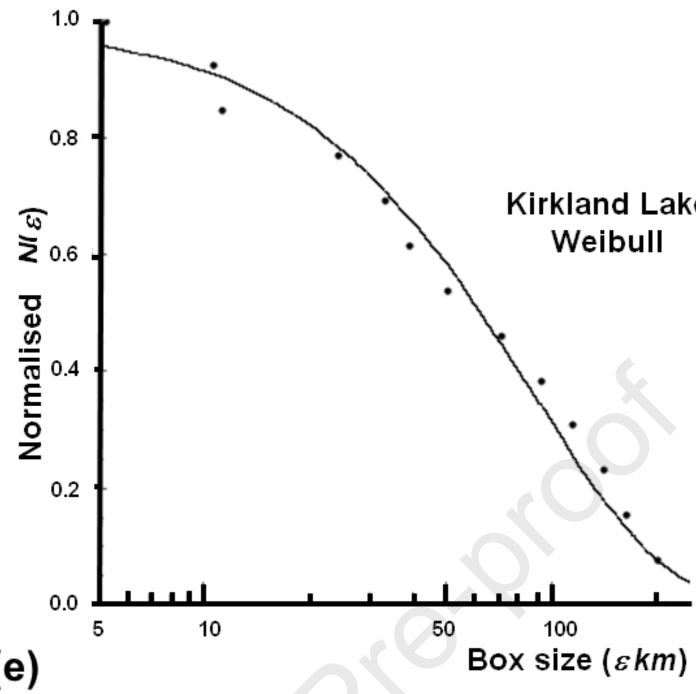
1.0
0.8
0.6
0.4
0.2
0.0
Normalised N(ε)
5
10
50
100
Box size (ε km)
Kirkland Lake
Weibull

(e)

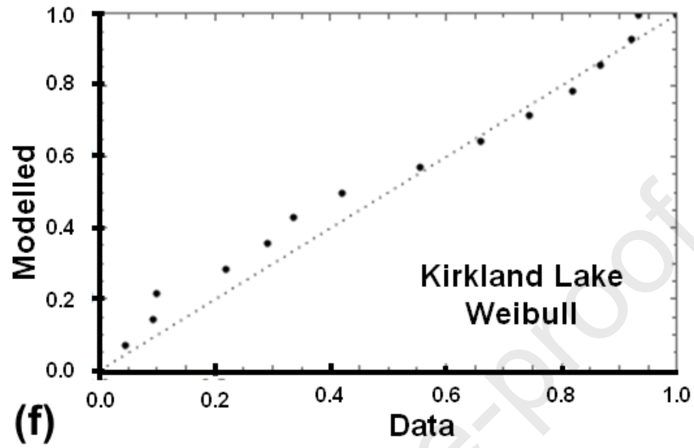
1.0
0.8
0.6
0.4
0.2
0.0
Modelled
0.0
0.2
0.4
0.6
0.8
1.0
Data
Kirkland Lake
Weibull
(f)

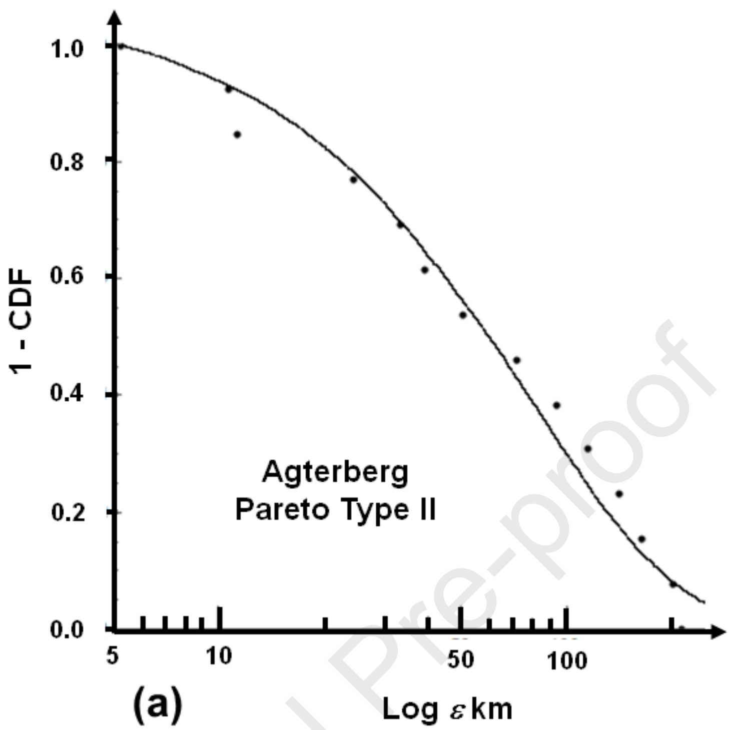
1.0
0.8
0.6
0.4
0.2
0.0
1 - CDF
Agterberg
Pareto Type II
5
10
50
100
(a)
Log ε km

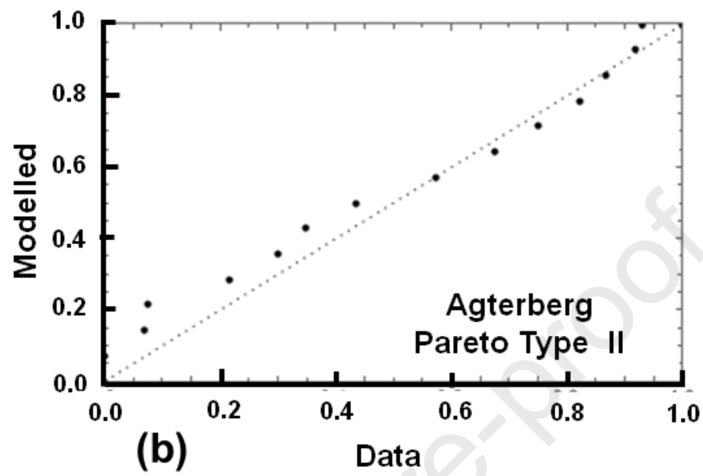
1.0
0.8
0.6
0.4
0.2
0.0
Modelled
Agterberg
Pareto Type II
0.0
0.2
0.4
0.6
0.8
1.0
(b)
Data

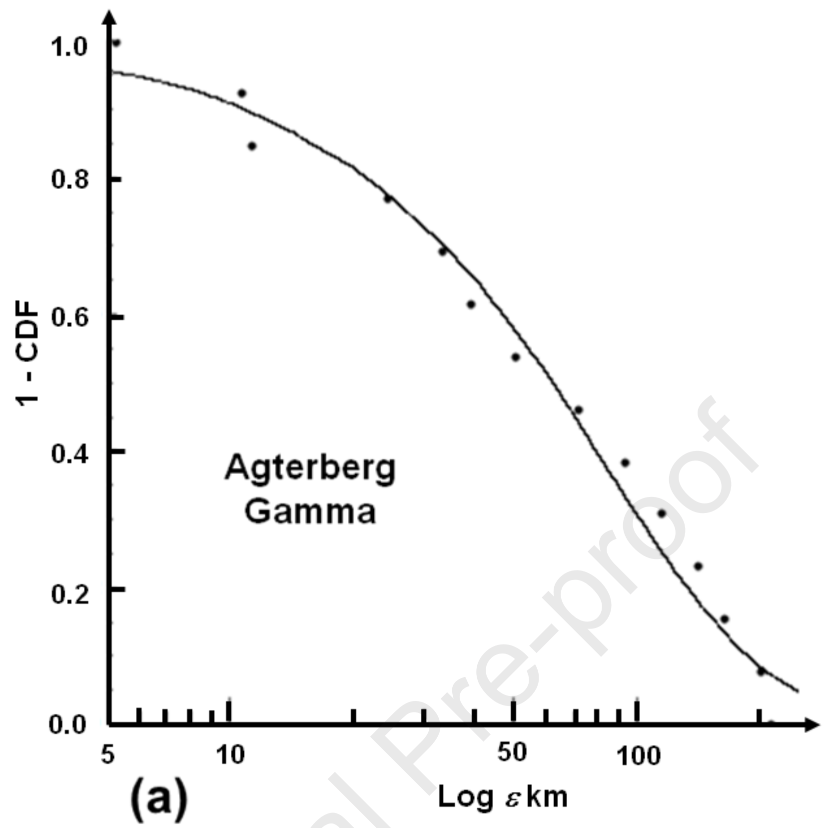
1.0
0.8
0.6
0.4
0.2
0.0
1 - CDF
Agterberg
Gamma
5
10
50
100
(a)
Log ε km

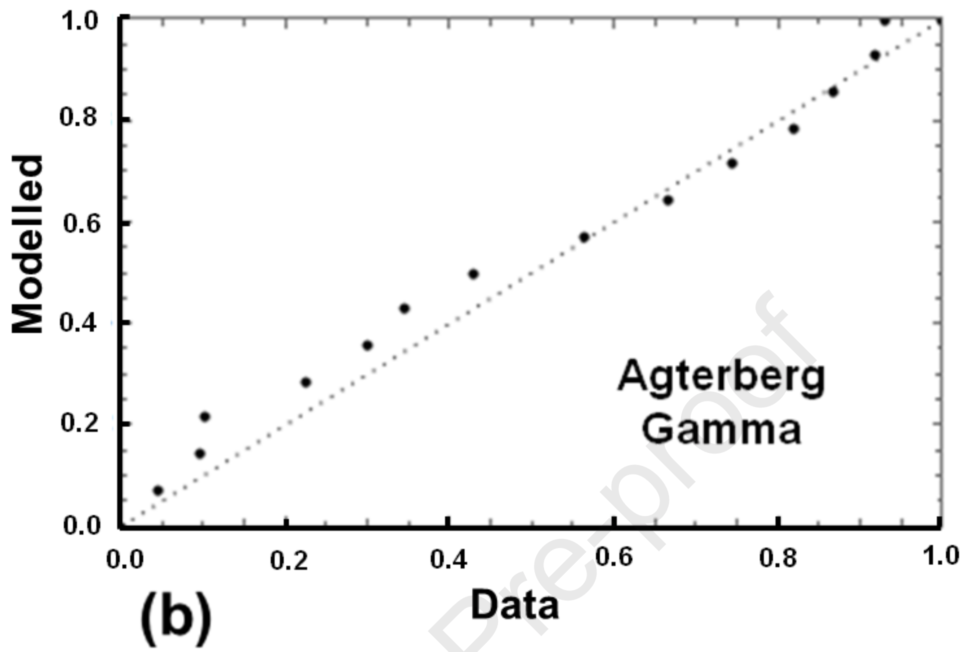
1.0
0.8
0.6
0.4
0.2
0.0
Modelled
0.0
0.2
0.4
0.6
0.8
1.0
Data
Agterberg
Gamma
(b)

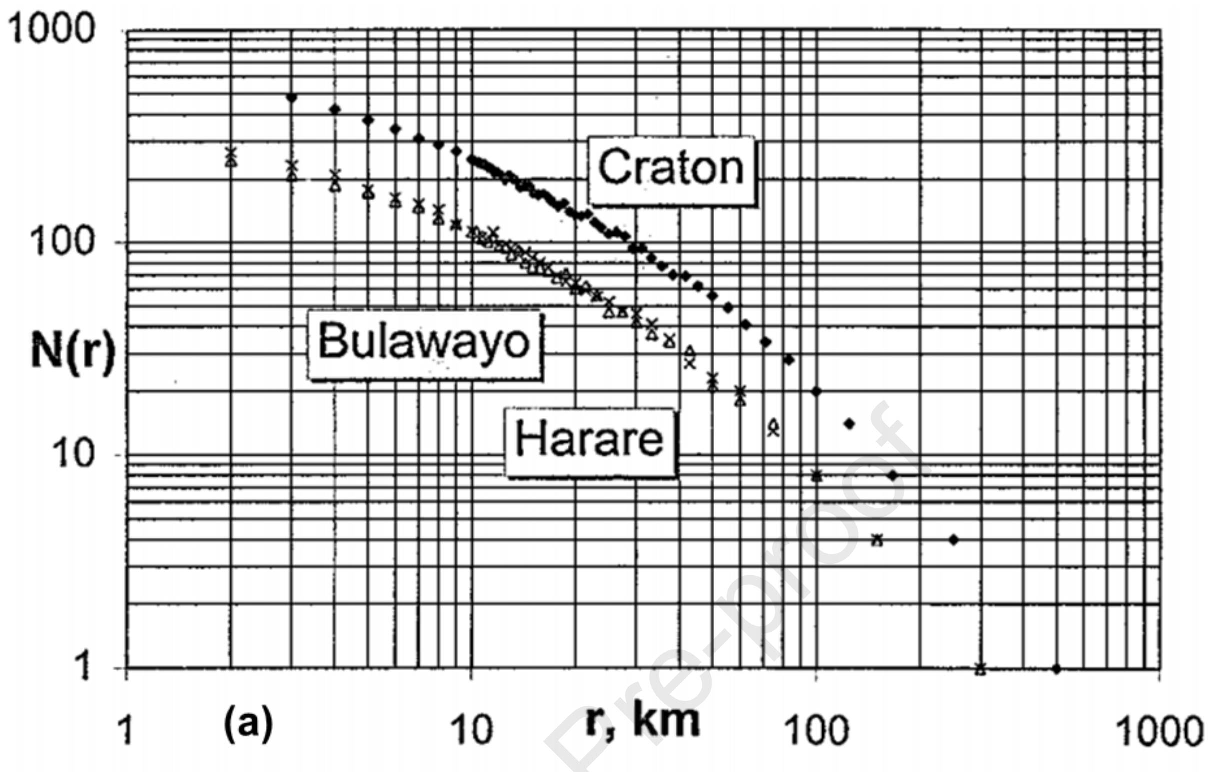
1000
100
10
1
N(r)
Craton
Bulawayo
Harare
1
(a)
10
r, km
100
1000

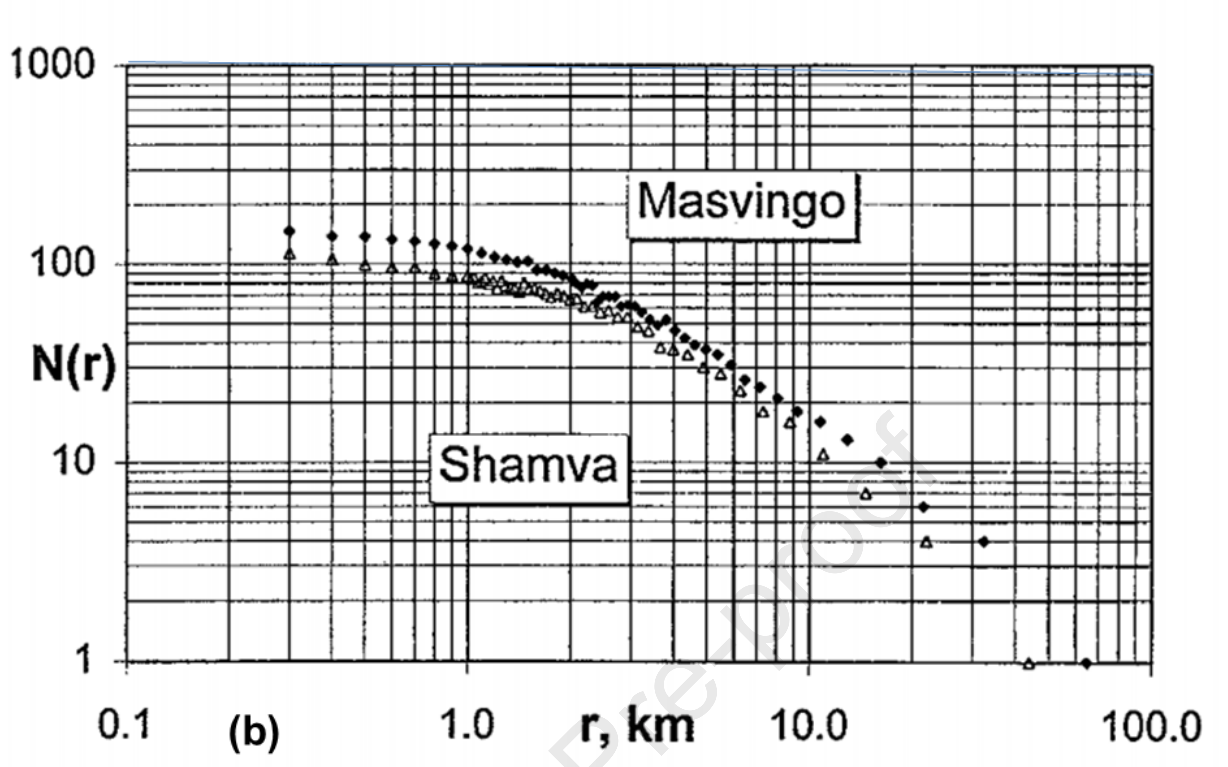
1000
100
N(r)
10
1
0.1
(b)
1.0
r, km
10.0
100.0
Masvingo
Shamva

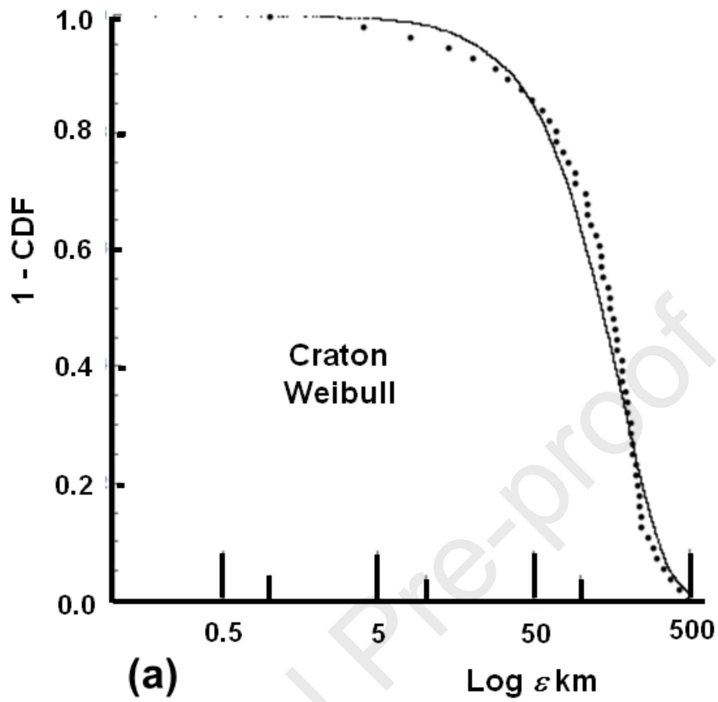
1.0
0.8
0.6
0.4
0.2
0.0
1 - CDF
Craton
Weibull
0.5
5
50
500
(a)
Log ε km

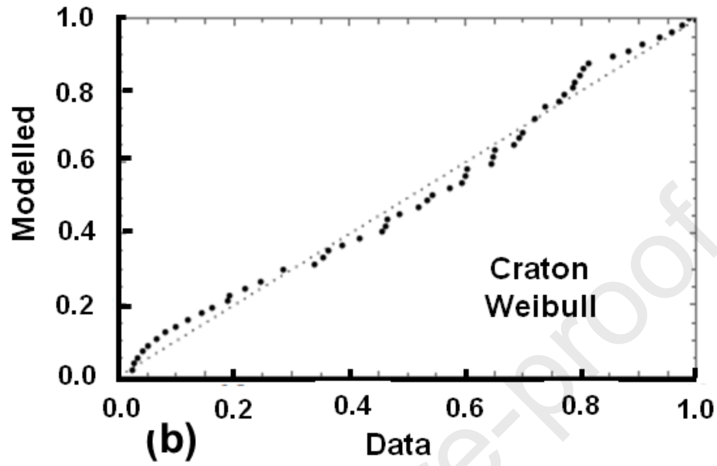
1.0
0.8
0.6
0.4
0.2
0.0
Modelled
0.0
0.2
0.4
0.6
0.8
1.0
Data
(b)
Craton
Weibull

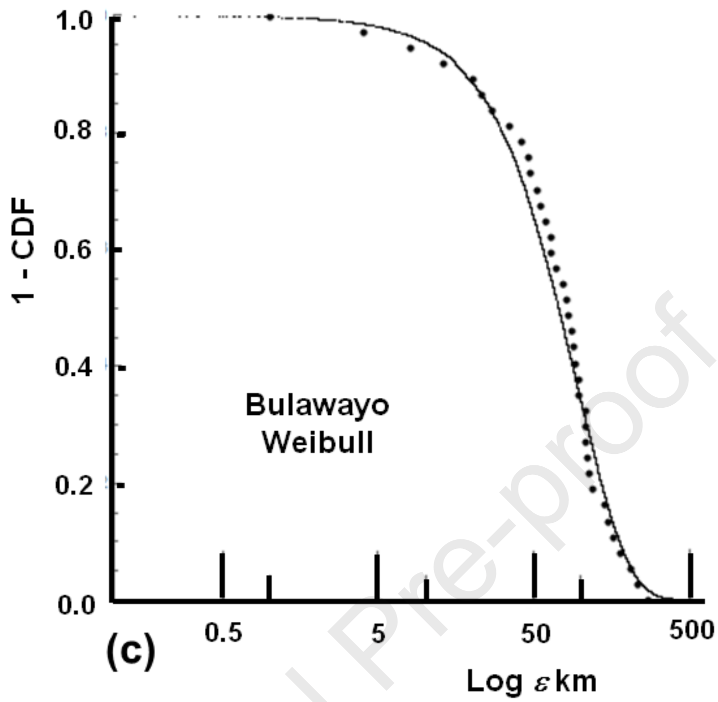
1.0
0.8
0.6
0.4
0.2
0.0
1 - CDF
Bulawayo
Weibull
0.5
5
50
500
(c)
Log ε km

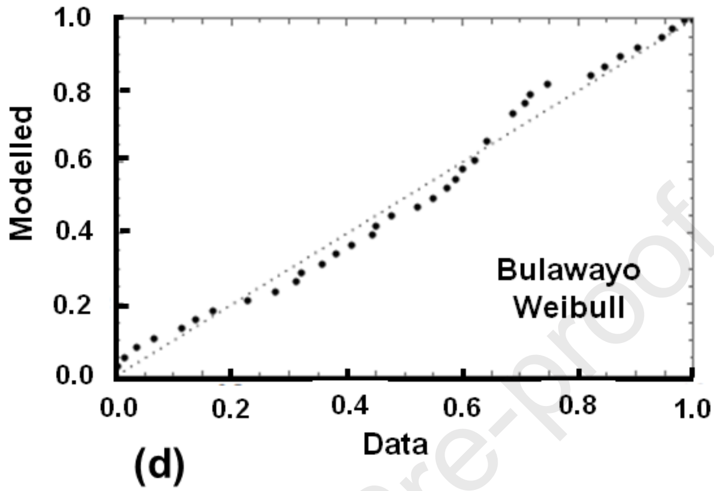
1.0
0.8
0.6
0.4
0.2
0.0
Modelled
0.0
0.2
0.4
0.6
0.8
1.0
Data
Bulawayo
Weibull
(d)

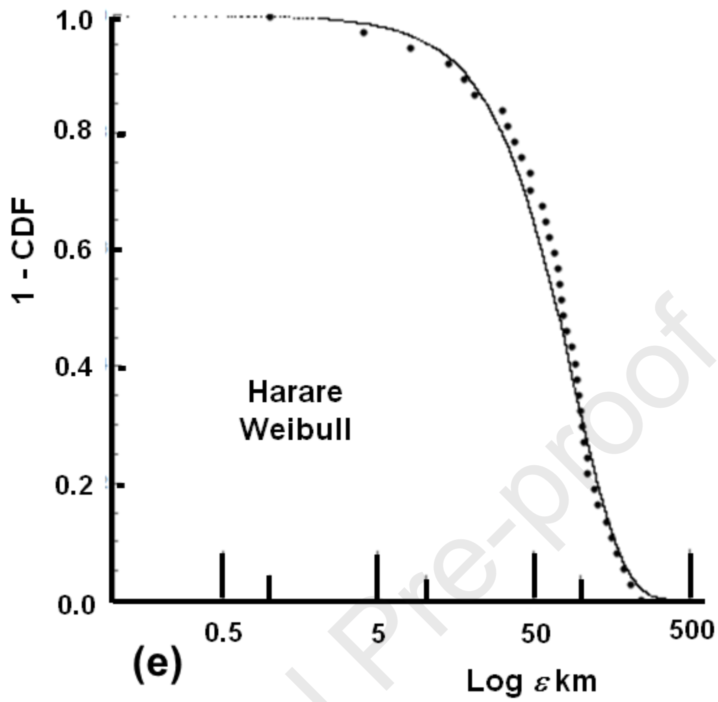
1.0
0.8
0.6
0.4
0.2
0.0
1 - CDF
Harare
Weibull
0.5
5
50
500
(e)
Log ε km

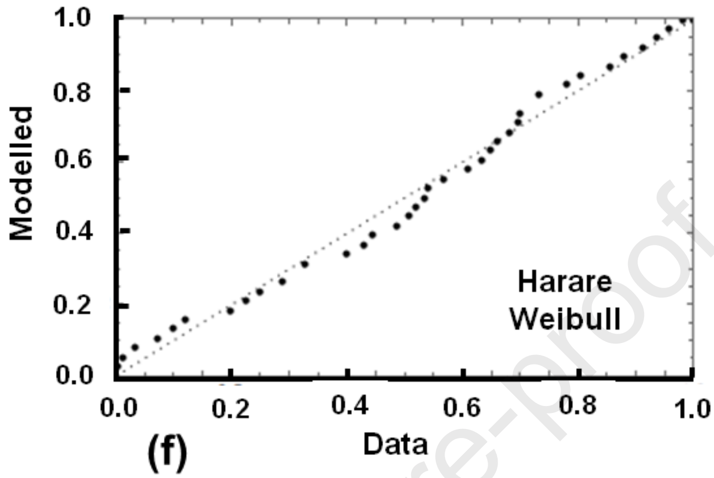

(f)

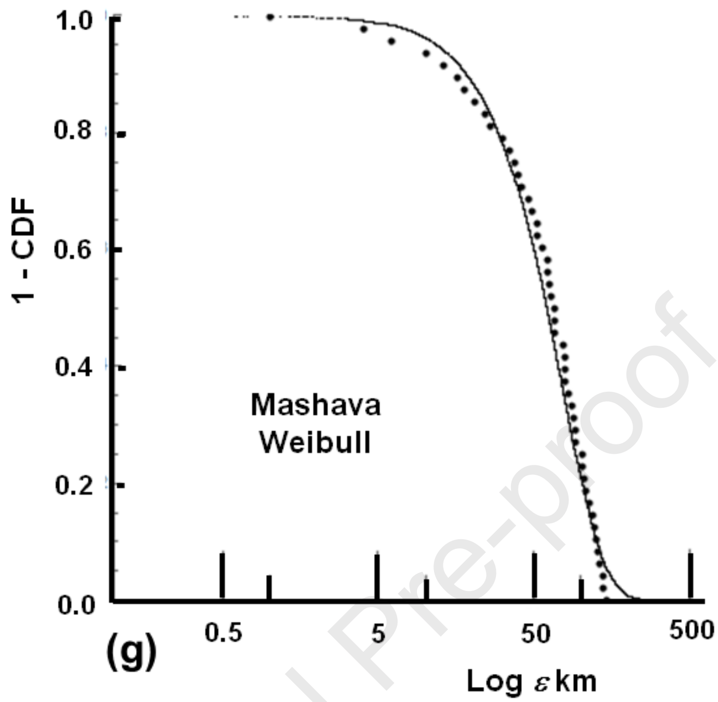
1.0
0.8
0.6
0.4
0.2
0.0
1 - CDF
Mashava
Weibull
0.5
5
50
500
(g)
Log ε km

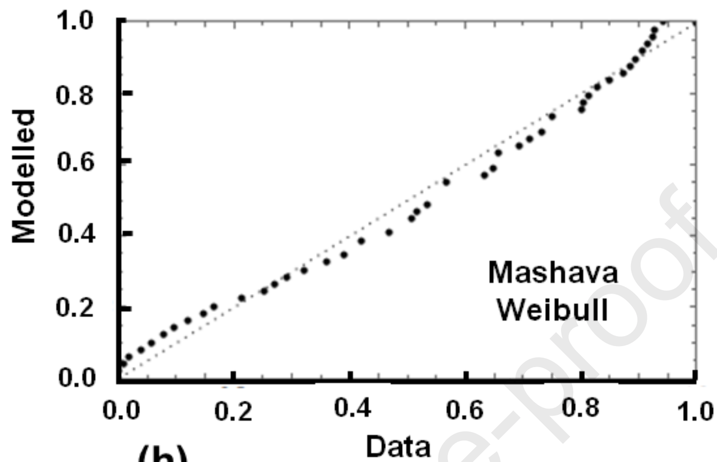
1.0
0.8
0.6
0.4
0.2
0.0
Modelled
0.0
0.2
0.4
0.6
0.8
1.0
Data
Mashava
Weibull

(h)

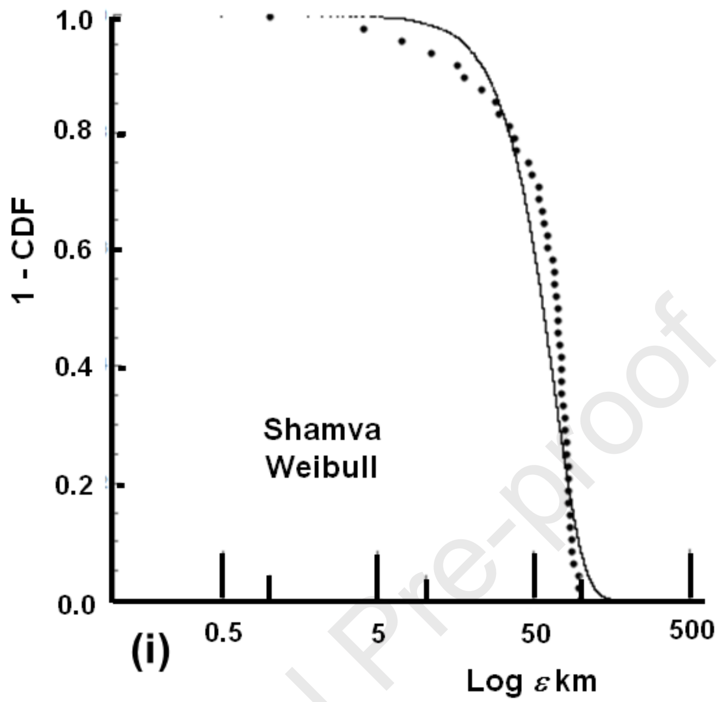
1.0
0.8
0.6
0.4
0.2
0.0
1 - CDF
Shamva
Weibull
0.5
5
50
500
(i)
Log ε km

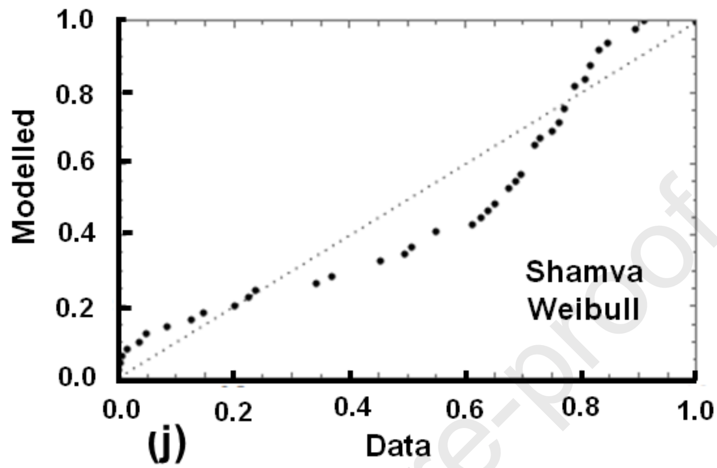
1.0
0.8
0.6
0.4
0.2
0.0
Modelled
0.0
0.2
0.4
0.6
0.8
1.0
Data
(j)
Shamva
Weibull

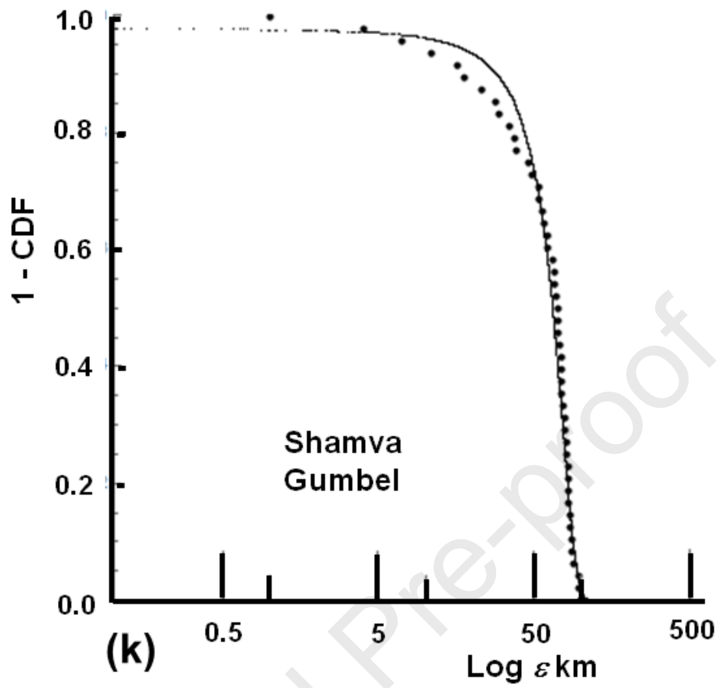
1.0
0.8
0.6
0.4
0.2
0.0
1 - CDF
Shamva
Gumbel
0.5
5
50
500
(k)
Log ε km

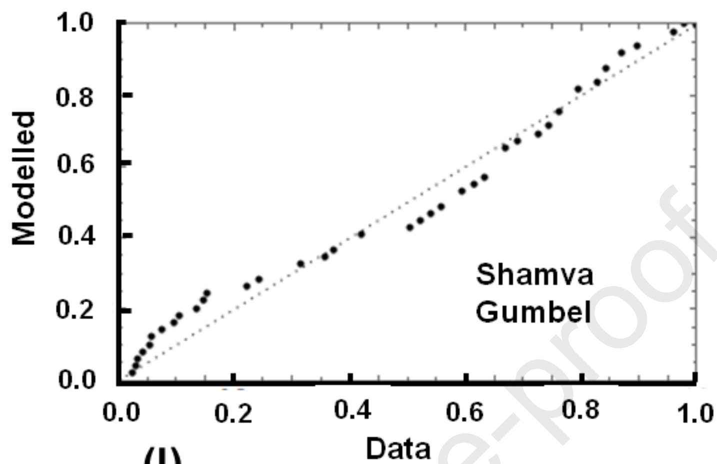

(l)

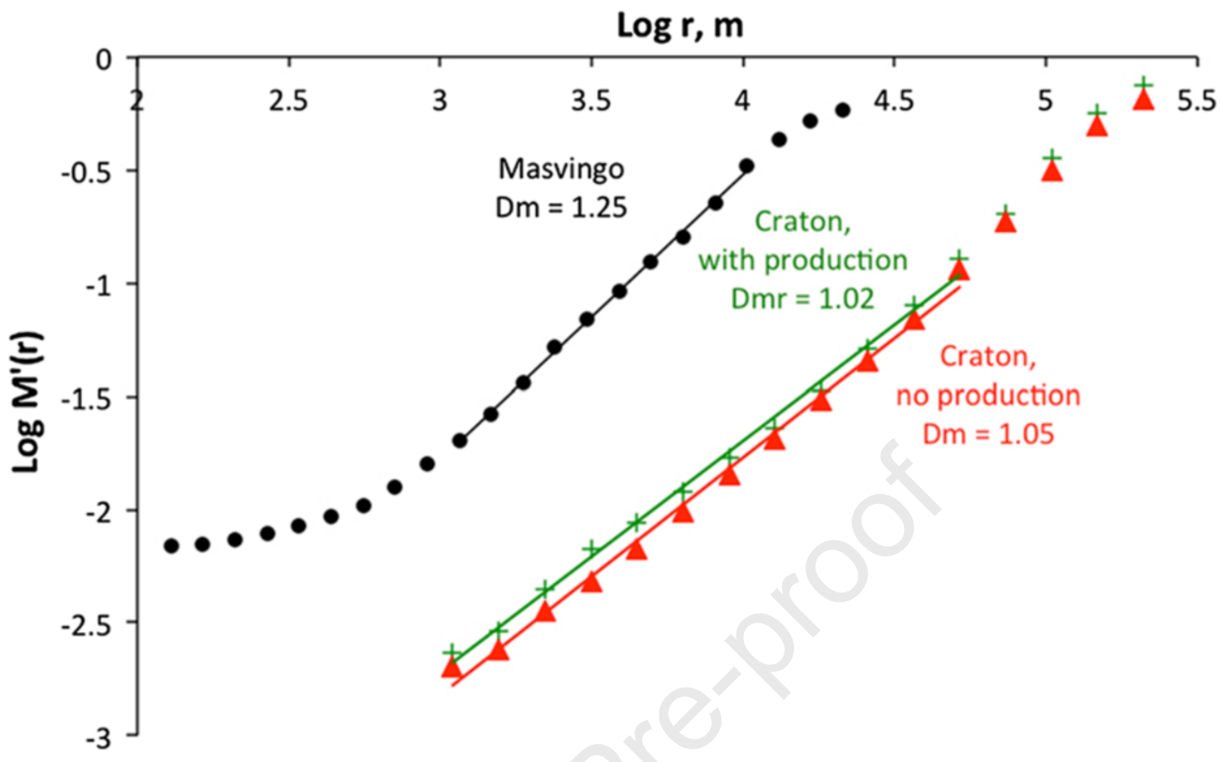
Log r, m
Log M'(r)
0
-0.5
-1
-1.5
-2
-2.5
-3
2
2.5
3
3.5
4
4.5
5
5.5
Masvingo
Dm = 1.25
Craton,
with production
Dmr = 1.02
Craton,
no production
Dm = 1.05

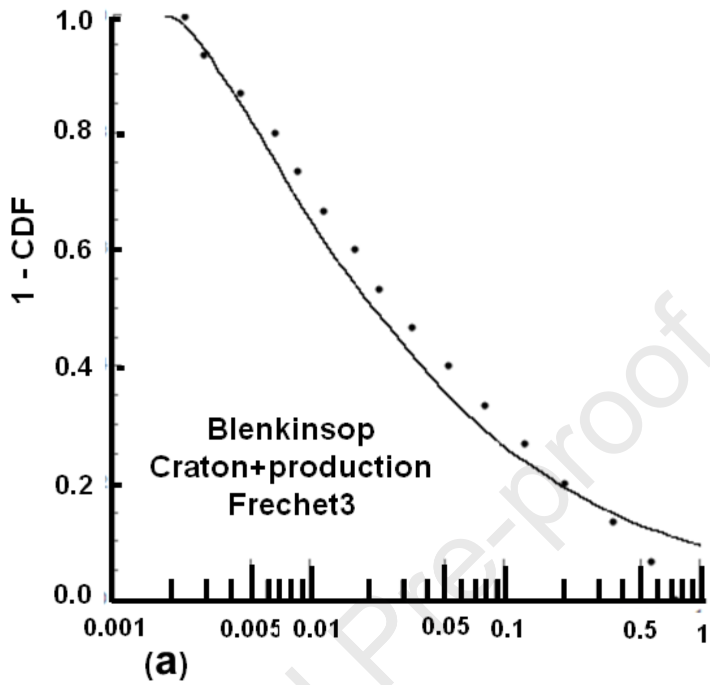
1.0
0.8
0.6
0.4
0.2
0.0
1 - CDF
Blenkinsop
Craton+production
Frechet3
0.001
0.005
0.01
0.05
0.1
0.5
1
(a)

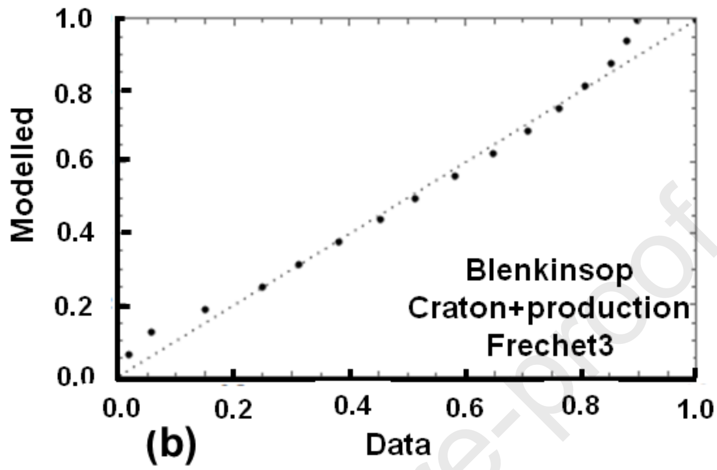
1.0
0.8
0.6
0.4
0.2
0.0
Modelled
Blenkinsop
Craton+production
Frechet3
0.0
0.2
0.4
0.6
0.8
1.0
(b)
Data

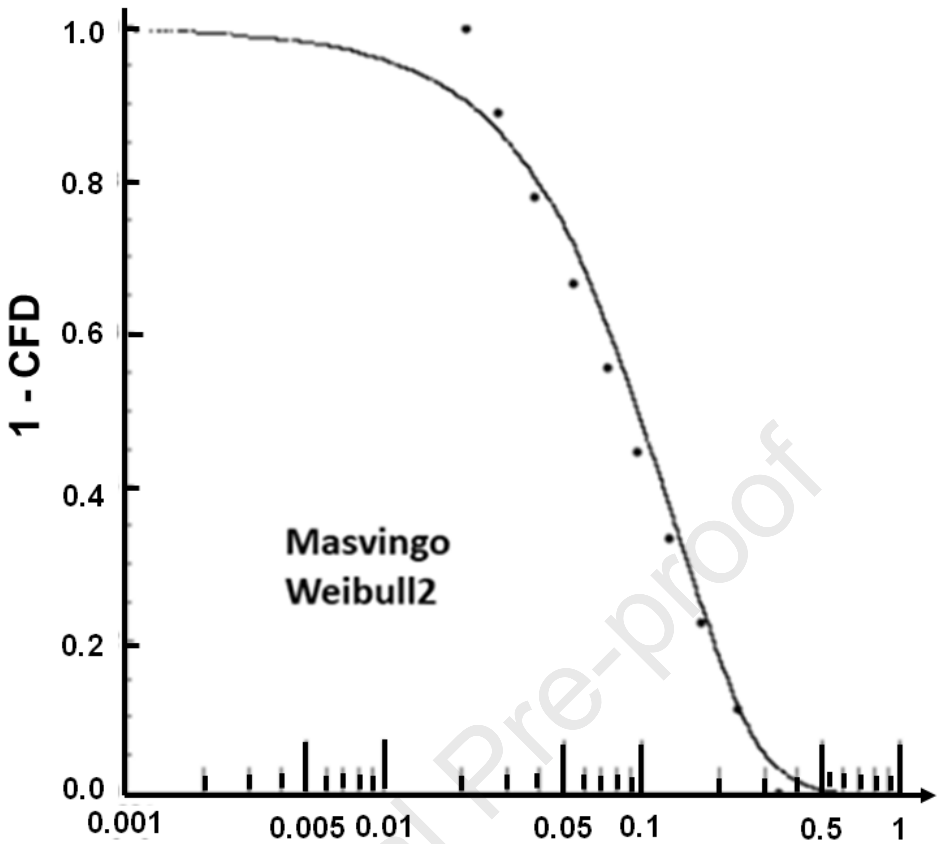
1 - CFD
1.0
0.8
0.6
0.4
0.2
0.0
Masvingo
Weibull2
0.001
0.005
0.01
0.05
0.1
0.5
1

(a)

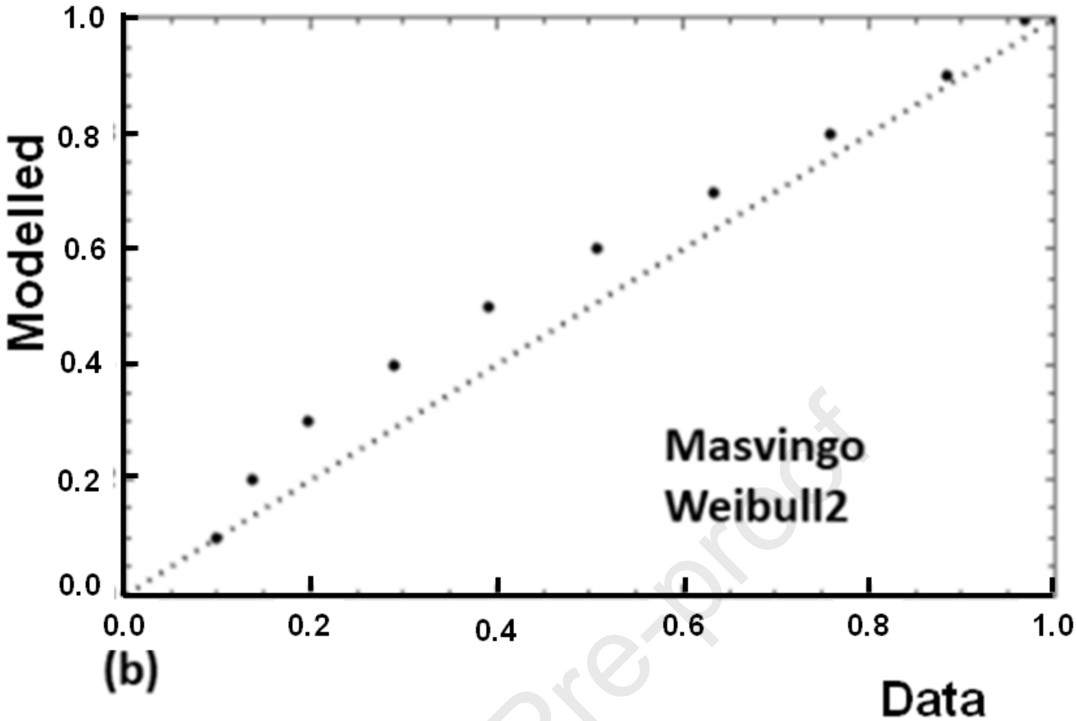
Modelled
1.0
0.8
0.6
0.4
0.2
0.0
0.0
0.2
0.4
0.6
0.8
1.0
Masvingo
Weibull2
Data

(b)

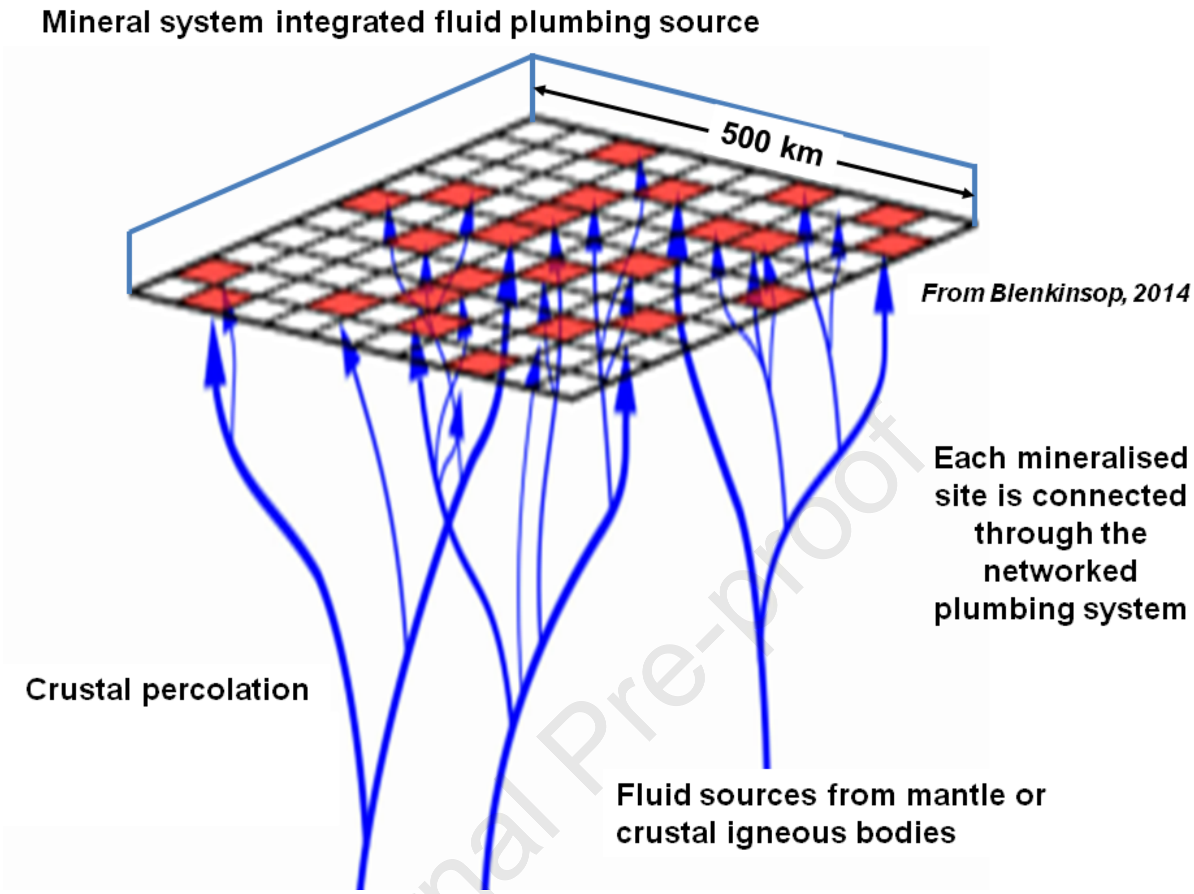
Mineral system integrated fluid plumbing source
500 km
From Blenkinsop, 2014
Each mineralised site is connected through the networked plumbing system
Crustal percolation
Fluid sources from mantle or crustal igneous bodies

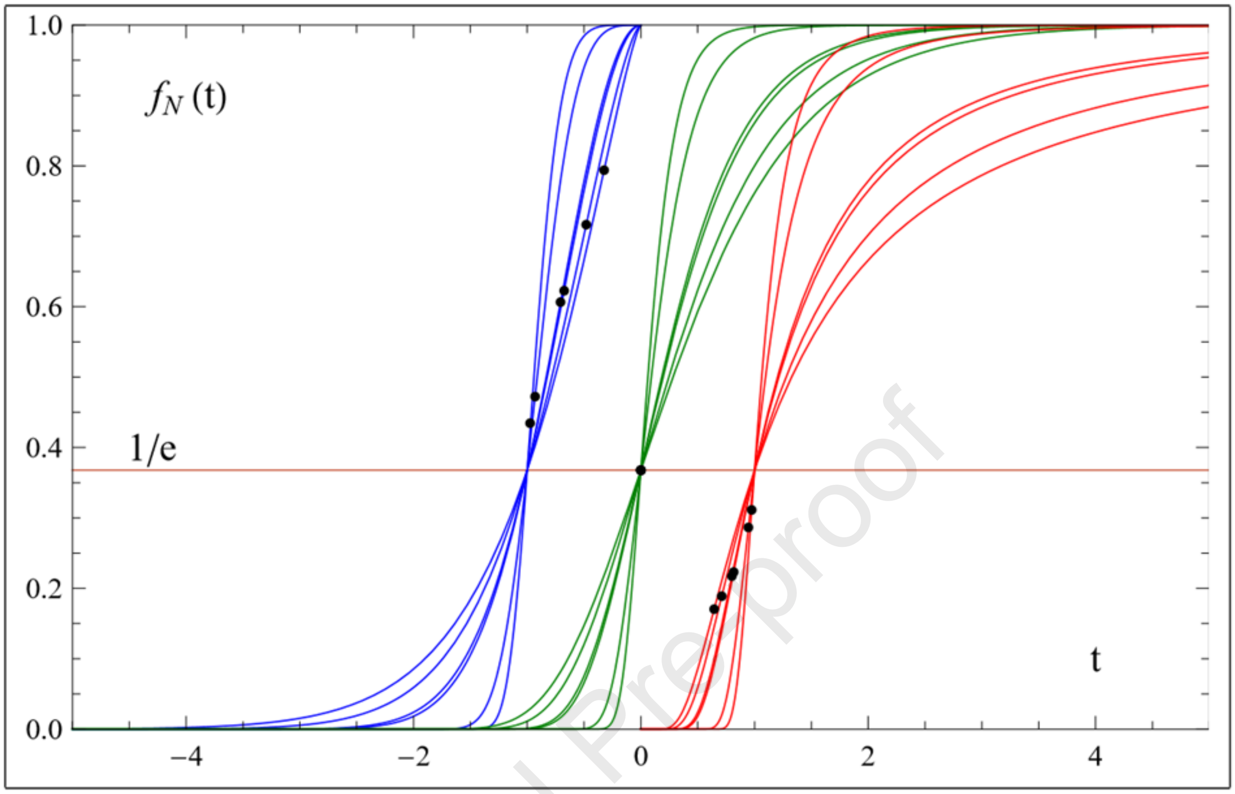
1.0
0.8
0.6
0.4
0.2
0.0
f_N (t)
1/e
t
−4
−2
0
2
4

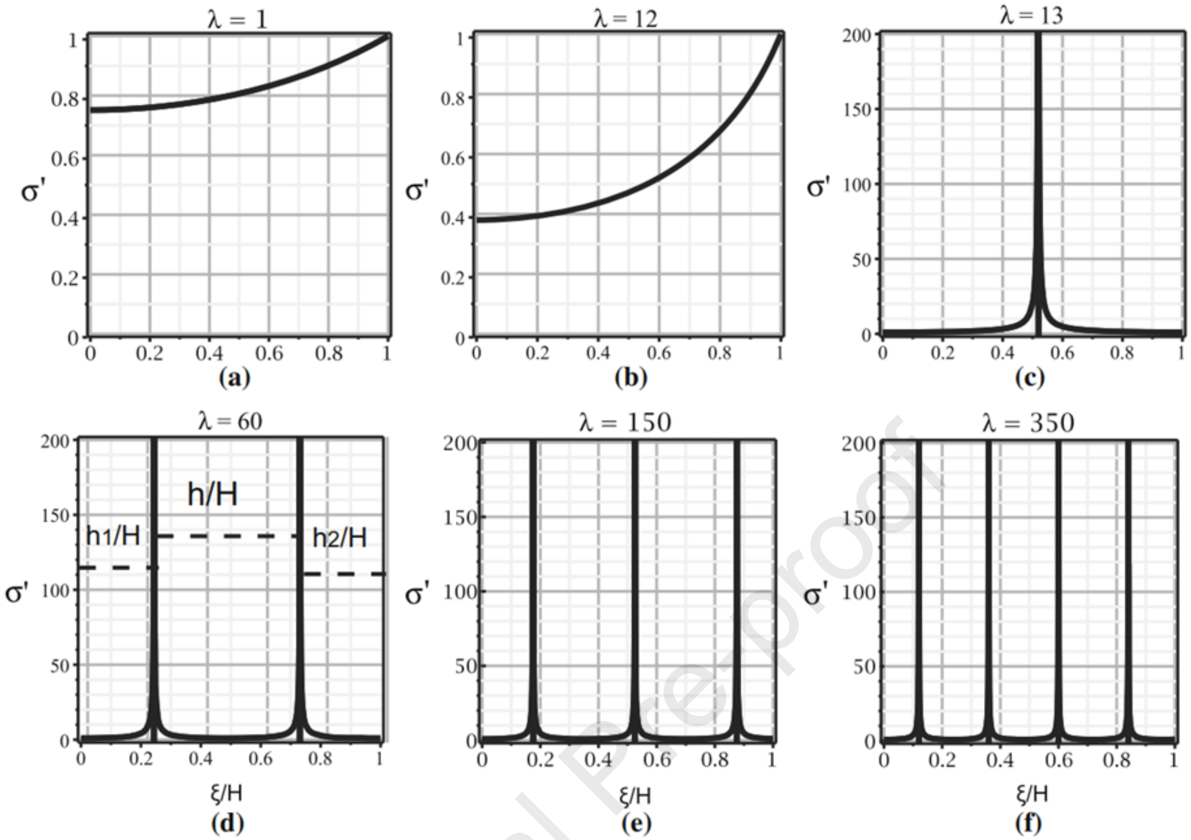
λ = 1
σ'
(a)
λ = 12
σ'
(b)
λ = 13
σ'
(c)
λ = 60
h/H
h1/H
h2/H
σ'
ξ/H
(d)
λ = 150
σ'
ξ/H
(e)
λ = 350
σ'
ξ/H
(f)

Highlights

- Mineralising systems are not fractal but Generalised Extreme Value distributions.
- Cumulative distributions are direct reflections of mineralising growth kinetics.
- Nucleation-growth-extinction systems may lead to GEV probability distributions.